University of Tehran

Earth Observation and Geomatics Engineering

Online ISSN: 2588-4360

Homepage: https://eoge.ut.ac.ir/

Assessing Regional Patterns of Post-Fire Vegetation Recovery, Degradation, and Change Using NDVI Time Series and MLP: A Multi-Region Case Study

Zohreh Roodsarabi [1], and **Mehdi Akhoondzadeh**[2]✉

1. Photogrammetry and Remote Sensing Department, School of Surveying and Geospatial Engineering College of Engineering, University of Tehran, North Amirabad Ave., Tehran 1417614411, Iran. E-mail: zohreh.roodsarabi@ut.ac.ir
2. Corresponding author, Photogrammetry and Remote Sensing Department, School of Surveying and Geospatial Engineering College of Engineering, University of Tehran, North Amirabad Ave., Tehran 1417614411, Iran. E-mail: makhonz@ut.ac.ir

Article Info

Article type:
Research Article

Article history:
Received 2025-07-27
Received in revised form 2025-10-07
Accepted 2025-10-17
Available 2026-05-12

Keywords:
Remote Sensing,
Satellite Time Series,
Deep Learning,
Vegetation Recovery Period,
Vegetation Recovery Rate.

ABSTRACT

Understanding regional variations in post-fire vegetation recovery is essential for enhancing forest resilience and informing land management under changing climatic conditions. This study combines multi-source satellite time series, including NDVI, EVI, SAVI, NBR, LST, ET, and drought indices, within a Google Earth Engine workflow and applies a Multi-Layer Perceptron neural network to model post-fire vegetation dynamics across twelve wildfire events in the United States and Spain between 2000 and 2022. The model achieved high predictive accuracy, with R^2 values exceeding 0.95 and RMSE values below 0.015 across all sites, including independent test fires, demonstrating its capacity to capture non-linear and region-specific recovery patterns. Two quantitative indicators—Vegetation Recovery Rate and Vegetation Recovery Period at 50, 70, and 90 percent of pre-fire NDVI—revealed pronounced heterogeneity among ecosystems. Some forested regions recovered within two to five years with VRR values up to 0.035, whereas Mediterranean and semi-arid areas displayed extended or negative recovery trends with VRR values as low as −0.009 and VRP90 reaching approximately 12 years. Results showed substantial variability in recovery trajectories driven by ecosystem type, climat,e and fire severity. While forested regions exhibited faster recovery, Mediterranean and semi-arid ecosystems experienced prolonged recovery or degradation trends. This framework provides a scalable and transferable approach for monitoring post-disturbance vegetation resilience using multi-source satellite time series and deep learning, with significant implications for post-fire restoration, adaptive management, and climate-informed decision making.

Cite this article: Roodsarabi, Z., Akhoondzadeh, M. (2025). Assessing Regional Patterns of Post-Fire Vegetation Recovery, Degradation, and Change Using NDVI Time Series and MLP: A Multi-Region Case Study. *Earth Observation and Geomatics Engineering*, Volume 9, Issue 1, Pages 23-46. http//doi.org/ 10.22059/eoge.2025.399556.1184

Publisher: University of Tehran.

DOI: http//doi.org/ 10.22059/eoge.2025.399556.1184

1. Introduction

Forest ecosystems are critical for global biodiversity and climate regulation, hosting approximately 80% of terrestrial species (Toivonen et al. 2023) and serving as major carbon sinks (Xu et al. 2024). However, these ecosystems face escalating threats from wildfires (Carta et al. 2023), which have intensified due to climate change-induced factors such as prolonged droughts, rising temperatures, and reduced fuel moisture (Chuvieco et al. 2014; Gilroy et al. 2014; Ramo and Chuvieco 2017). While fires are a natural component of many ecological cycles, promoting regeneration and species diversity (Kelly and Brotons 2017), their increasing frequency and severity disrupt forest structure, carbon sequestration, and ecosystem services (Anderegg et al. 2020). At the global scale, fires alter atmospheric chemistry (Knorr, Jiang, and Arneth 2016), impact forest succession and health (Merrill et al. 2018), and contribute to carbon budget shifts and land use changes (Chuvieco et al. 2019). These impacts are particularly pronounced in fire-prone regions such as Mediterranean, arid, and semi-arid ecosystems, where the combined ecological and socioeconomic consequences highlight the urgent need for effective monitoring and management strategies (San-Miguel-Ayanz et al. 2022).

The trajectory of post-fire vegetation recovery directly influences surface energy balance, albedo, soil moisture, erosion, and evapotranspiration parameters that collectively impact climate regulation (Jeong et al. 2011; Jiang and Liang 2013; Zou et al. 2020). Furthermore, the structure and function of recovering vegetation are central to restoring ecosystem services, habitat integrity, and species reestablishment (Arthur, Catling, and Reid 2012; Gimeno-García, Andreu, and Rubio 2007). In arid and semi-arid regions, such as parts of the United States, Spain, and Saudi Arabia, harsh environmental conditions exacerbate the challenges of vegetation regeneration, threatening biodiversity, soil stability, and water availability (Bayoumi et al. 2018; El-Rawy et al. 2023). Regions at higher latitudes are experiencing pronounced warming effects, leading to increased fire activity and prolonged recovery periods (Girardin 2007; Marlon et al. 2008). Consequently, post-fire regeneration and long-term ecosystem stability are emerging as key priorities in both ecological research and forest management planning (Chen, Zhao, and Guo 2010; Gilroy et al. 2014).

Remote sensing (RS) has emerged as a powerful and cost-efficient tool for monitoring wildfire impacts and vegetation recovery, offering high-resolution spatial and temporal data to track ecosystem dynamics (Hawe and Fuquay 1969; Kourtz 1968). While early research on post-fire vegetation recovery largely relied on labor-intensive field surveys, RS has since become indispensable for overcoming the limitations of traditional methods (Llorens et al. 2021; Sun et al. 2019). Cloud-based platforms such as Google Earth Engine (GEE) are now powerful resources for RS applications by providing access to diverse Earth observation datasets, enabling large-scale processing and analysis in studies of land resources and wildfires (Gorelick et al. 2017; He et al. 2023; Kennedy et al. 2018). Various optical spectral indices derived from satellite imagery, particularly from Landsat series (Gorelick et al. 2017; Kennedy et al. 2018) and Moderate Resolution Imaging Spectroradiometer (MODIS) sensors (Helman et al. 2015; Joao et al. 2018), are commonly employed to quantify post-fire vegetation recovery by measuring changes in greenness and biomass (Ba et al. 2022; Vanderhoof et al. 2021; Zhang et al. 2023; Zhijie 2024). Among these, the Normalized Difference Vegetation Index (NDVI) is the most prominent, serving as a key indicator of plant growth and ecosystem change (Goward, Tucker, and Dye 1985; Johnstone et al. 2016; Pausas and Keeley 2019). Nevertheless, NDVI alone may underestimate post-fire structural recovery due to its saturation in dense canopies and sensitivity to soil background effects (Hao et al. 2022; Lopes et al. 2024). Recent advances in structural remote sensing—such as GEDI LiDAR canopy height and biomass products (Dubayah et al. 2020), airborne LiDAR surveys (Toivonen et al. 2023), and radar-based vegetation structure indices—have demonstrated potential to overcome these limitations. While these datasets provide valuable insights into vertical canopy structure and biomass accumulation, they often lack the long-term temporal coverage required for multi-decadal fire recovery studies. For this reason, the present study focuses on long-term spectral indices derived from MODIS data, while recognizing that future work should integrate structural datasets to achieve a more comprehensive understanding of ecosystem recovery.

Post-fire vegetation recovery is a complex process governed by multiple environmental and ecological factors, including fire severity, vegetation type, local climate, topography, proximity to unburned areas, and species resilience (Bassett et al. 2017; Gilroy et al. 2014; Marlon et al. 2013; Merrill et al. 2018). These intrinsic factors, combined with land management and climate adaptation policies, determine the resulting recovery trajectories, which can vary significantly from a few years in Mediterranean shrublands to decades in boreal forests (Banskota et al. 2014) Ecosystem recovery plays a critical role in global and regional processes by influencing surface radiation balance, carbon budgets, water balance, albedo, soil moisture, erosion, and evapotranspiration. Furthermore, successful recovery supports ecological function restoration, species habitat recovery, and biota recolonization (Jeong et al. 2011; Jiang and Liang 2013; Zou et al. 2020). Quantifying the interplay between climate and vegetation recovery remains essential for sustainable forest management, as this information is crucial for designing effective interventions to enhance ecosystem resilience and mitigate climate impacts (Davis et al. 2019; Larson et al. 2022; Stevens, Safford, and Latimer 2014). Therefore, the integration of NDVI with other environmental factors and advanced RS tools like GEE offers a robust framework for monitoring and managing post-fire vegetation recovery across diverse

ecosystems.

Recent advancements in machine learning (ML) and deep learning (DL) have revolutionized the analysis of post-fire vegetation dynamics, providing powerful tools for early warning systems, risk assessment, and long-term ecological monitoring (Reichstein et al. 2019; Rolnick et al. 2022). DL models, particularly deep neural networks, excel at extracting high-level features from raw spatiotemporal data, enabling the detection of complex, non-linear patterns that traditional index-based methods often overlook (Learning 2016; LeCun, Bengio, and Hinton 2015). These capabilities are especially valuable in fire-prone and topographically complex regions, where conventional approaches such as dNBR may suffer from inaccuracies due to sensor limitations or insufficient temporal resolution (Alonso-González and Fernández-García 2021; Cardil et al. 2021). By integrating multi-source satellite data from platforms like MODIS and Landsat via GEE, ML models can leverage large-scale, long-term environmental records to significantly improve fire impact assessment and recovery forecasting (Abid 2021; Hird, Kariyeva, and McDermid 2021). The autonomous feature learning and adaptive nature of ML algorithms render them particularly suitable for studying dynamic ecosystems, where interactions between vegetation indices, climate variables, and temporal dynamics are intricate and non-stationary (Karpatne et al. 2018; Shen 2018).

Despite these advances, significant gaps persist in fully understanding the long-term, heterogeneous patterns of post-fire vegetation recovery across diverse global biomes, particularly in arid and mountainous regions (Bayoumi et al. 2018; Libonati et al. 2021). Many previous studies have relied predominantly on linear models or single-index analyses, which are insufficient to accurately capture the complex, non-linear dynamics inherent in post-fire recovery processes. To comprehensively address the limitations of traditional approaches, recent research has increasingly explored advanced ML/DL architectures and multi-sensor data fusion to better quantify fire impacts and recovery trajectories across spatial and temporal scales.

For instance, (Qiu et al. 2021) applied Random Forest (RF) and Support Vector Machine (SVM) models to quantify post-fire vegetation recovery in northeastern China, demonstrating that topography, temperature, and precipitation jointly influence regrowth speed. Similarly, (Liu et al. 2025) compared several ML algorithms in complex mountainous regions and found that RF outperformed other classifiers (overall accuracy =0.90) in mapping fire severity and characterizing distinct recovery trajectories. Furthermore, (Al-Qthanin and Aseeri 2025) utilized RF regression combined with Landsat 8, Sentinel−2, and DEM data to model recovery in Saudi Arabia's semi-arid mountains, emphasizing the dominant role of pre-fire vegetation density and moisture (NDWI) in determining recovery potential.

More advanced DL-based approaches have emerged in recent years. (Priya and Vani 2024) developed a Deep Embedded Clustering (DEC) and Adaptive Generative Adversarial Network (AdaptiGAN) framework, achieving 96.17% accuracy in identifying post-fire vegetation change and re-vegetation patterns. Similarly, (Simpson et al. n.d.) implemented multi-task LSTM and ConvLSTM architectures to forecast NDVI and LAI trajectories across western U.S. fires, revealing strong capabilities in modeling long-term vegetation recovery. (AnjanaDevi, Praveen, and Ramanathan 2024) presented a hybrid CNN–RNN model that integrates spectral, meteorological, and terrain data for predicting vegetation regrowth and soil chemistry after wildfire, showing improved temporal consistency compared to conventional ML models.

In the Mediterranean region, (Souane et al. 2024) utilized Random Forest and LANDIS-II simulations to analyze multi-year post-fire dynamics in Algerian forests, integrating climate, topography, and spectral indices to achieve 70% accuracy. (Zahabnazouri et al. 2025) used Sentinel−2–derived dNBR and dNDVI to compare recovery in burned and repeatedly burned zones of southern Italy, showing that repeated fires slow down regeneration and can shift forests toward shrublands. Similarly, (Wang et al. 2025) examined post-fire recovery in Siberian dwarf pine shrublands, reporting that slope, aspect, and soil moisture strongly regulate regeneration rates, while (Wassner, Figueiredo, and Nunes 2025) found that soil and species composition outweighed fire severity in driving recovery across Mediterranean Portugal.

Collectively, these studies reveal rapid progress in ML/DL applications for post-fire analysis but expose key limitations: most focus on a single region or a limited set of indices (e.g., NDVI or NBR), and few integrate comprehensive multi-sensor and climatic variables within a unified deep learning framework across geographically diverse biomes. To bridge these gaps, the present study employs a Multi-Layer Perceptron (MLP) architecture that integrates a broad suite of spectral (NDVI, EVI, SAVI, NBR), thermal (LST, ET), and climatic (SPEI, precipitation, temperature, and soil moisture) indicators derived from monthly averaged time series data (2000–2022). This framework is utilized to quantify and compare vegetation recovery, degradation, and resilience across twelve wildfire events spanning diverse ecosystems in the United States and Spain.

The model was trained on a composite dataset derived from nine fire events and was rigorously validated on three independent test fires (Thomas, King, Zaca Fires), thereby ensuring robust generalization. To effectively prevent overfitting, the architecture incorporates L2 regularization and dropout layers, while MinMaxScaler normalization ensures numerical stability across input features. Post-fire recovery is quantitatively assessed using Sen's Slope (referred to as the Vegetation Recovery Rate (VRR)) and the Vegetation Recovery Period (VRP) at 50%, 70%, and 90% thresholds of the pre-fire baseline NDVI, providing a nuanced understanding of recovery speed and ecological resilience. This integrated ML-based framework offers a

scalable, data-driven approach for monitoring ecological recovery, supporting critical land management decisions, and enhancing predictive capabilities in fire-affected landscapes worldwide.

The article is organized into six distinct sections. Section 2 details the study areas and data sources, Section 3 outlines the MLP methodology and the specific recovery metrics, Section 4 presents the quantitative results, including model performance and recovery trajectories, Section 5 discusses the ecological implications and compares findings with prior studies, and Section 6 concludes with management recommendations and future research directions.

2. Study Area and Data

2.1 Study Area

This study investigates twelve major wildfire events across the United States and Spain, which were specifically selected due to their occurrence in fire-prone arid, semi-arid, and Mediterranean-climate regions (Figure 1). The U.S. sites, located in California, Colorado, and Texas, represent a significant range of climatic conditions: Mediterranean along California's coast, semi-arid in Colorado, and dry continental in central Texas (NOAA 2024; Peel, Finlayson, and McMahon 2007). These regions host diverse ecosystems, including coniferous forests, chaparral, and grasslands, which are critical for studying post-fire vegetation recovery using NDVI time series (Steel, Safford, and Viers 2015). The Spanish site in the Valencia region features a Mediterranean climate with hot, dry summers and is dominated by shrub ecosystems prone to recurrent wildfires (Viedma, Moity, and Moreno 2015). The wildfires, which range in size from 2,900 to 405,000 ha, were selected based on their ecological significance, the availability of high-resolution RS data, and their diverse climatic drivers (Table 1). This multi-region approach enables a robust comparative analysis of post-fire vegetation dynamics across widely varying environmental conditions.

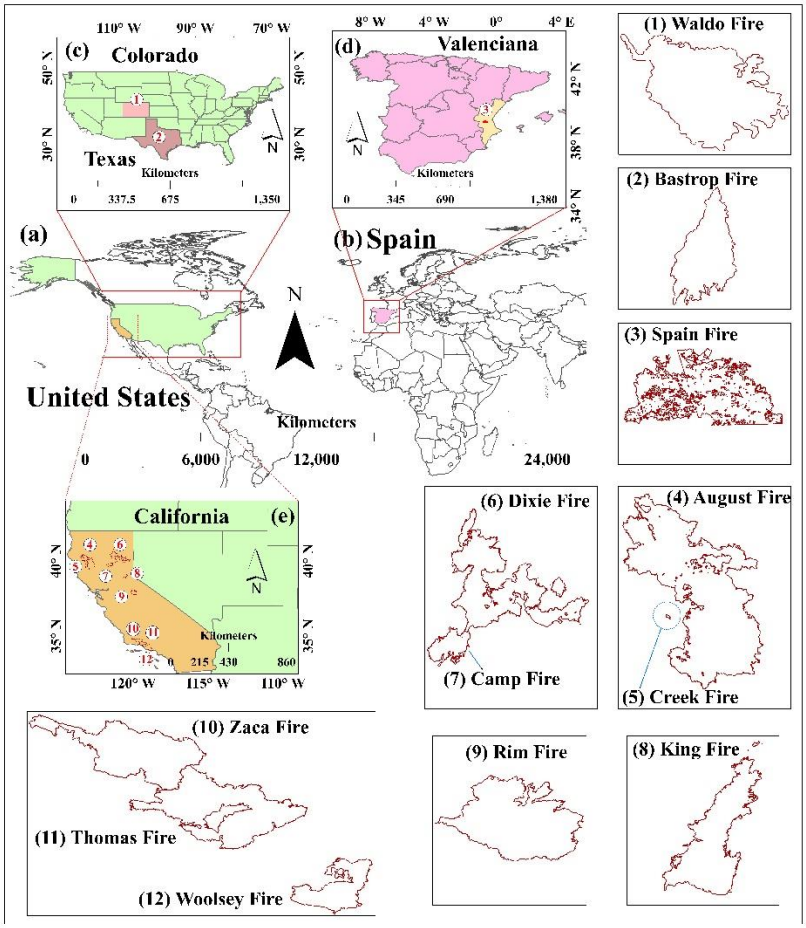

Figure 1. Locations of the twelve studied wildfire sites in (a) the United States and (b) Spain. The fire perimeters in (c) Colorado and Texas, (d) the Valencia region of Spain, and (e) California. Numbers correspond to: (1) Waldo Canyon Fire, (2) Bastrop County Fire, (3) Spain Fire, (4) August Complex Fire, (5) Creek Fire, (6) Dixie Fire, (7) Camp Fire, (8) King Fire, (9) Rim Fire, (10) Zaca Fire, (11) Thomas Fire, (12) Woolsey Fire.

Table 1. Characteristics of the studied wildfires in the United States and Spain.

NO.	Fire Name	Location	Start Date	Burned Area	Refrence
1	**Waldo Canyon Fire**	Colorado (near Colorado Springs)	June 23, 2012	7,400 ha (18,286 acres)	(Keeley and Syphard 2016)
2	**Bastrop County Fire**	Texas (Bastrop County)	September 4, 2011	13,760 ha (34,000 acres)	(Bastrop County Complex 2012)
3	**Spain Fire**	Spain (Valencia region)	July 3, 2012	2,900 ha	(Viedma, Moity, and Moreno 2015)
4	**August Complex Fire**	Northern California	August 17, 2020	405,000 ha (1,000,000 acres)	(CAL FIRE 2020a)
5	**Creek Fire**	California (Sierra National Forest)	September 4, 2020	153,600 ha (379,895 acres)	(CAL FIRE 2020b)
6	**Dixie Fire**	Northern California	July 13, 2021	389,847 ha (963,309 acres)	(CAL FIRE 2021)
7	**Camp Fire**	California (Butte County)	November 8, 2018	62,053 ha (153,336 acres)	(CAL FIRE 2018a)
8	**King Fire**	California (El Dorado National Forest)	October 17, 2014	39,600 ha (97,717 acres)	(CAL FIRE 2014)
9	**Rim Fire**	California (Stanislaus National Forest)	August 17, 2013	104,131 ha (257,314 acres)	(van Gerrevink and Veraverbeke 2021)
10	**Zaca Fire**	California (Santa Barbara County)	July 4, 2007	97,000 ha (240,207 acres)	(CAL FIRE 2007)
11	**Thomas Fire**	California (Santa Barbara & Ventura Counties)	December 4, 2017	114,078 ha (281,893 acres)	(CAL FIRE 2017)
12	**Woolsey Fire**	California (Los Angeles & Ventura Counties)	November 8, 2018	39,268 ha (96,949 acres)	(CAL FIRE 2018b)

2.2. Remote Sensing Data Collection

The study utilizes an extensive suite of RS datasets and spectral indices to investigate the spatial and temporal dynamics of post-fire vegetation recovery. Unlike traditional approaches that rely primarily on a limited set of indicators such as NDVI and NBR (Kim et al. 2021; Martins et al. 2024; Teshaev, Inamov, and Juraev 2025), this methodology integrates multiple vegetation, water, drought, thermal, and climatic indices to capture a comprehensive picture of post-disturbance ecological processes. Monthly average time-series data from 2000 to 2022 were compiled and processed using GEE, a robust cloud-based platform that enables efficient access to multi-source satellite archives. Preprocessing procedures, including cloud masking and temporal aggregation, were applied to ensure data consistency and quality. The resulting dataset encompassed a broad range of indicators: vegetation indices (e.g., NDVI, EVI, SAVI, and their variants), burn severity metrics (e.g., NBR), water-related indices (e.g., NDWI, MNDWI, NMDI), thermal parameters (e.g., daytime and nighttime LST), and key climatic variables (e.g., precipitation, air temperature, soil moisture, and relative humidity). These variables serve as critical input features to the MLP model for predicting vegetation recovery patterns and transitions. The diverse selection of indices reflects the multifaceted nature of post-fire ecological succession, thereby enhancing the capacity to model vegetation regrowth, degradation, or shifts under varying environmental conditions.

NDVI, a foundational vegetation metric, utilizes red and near-infrared reflectance to estimate plant health and density (Tucker 1979). While widely employed due to its simplicity and effectiveness (Wilson and Norman 2018), NDVI is subject to limitations in areas with dense canopies or strong soil background influence. To mitigate this, EVI and EVI2 were included; these indices improve vegetation detection by correcting for canopy background and atmospheric aerosol influences, making them particularly valuable in ecological studies and time-series analysis (Huete et al. 2002; Jiang et al. 2008). The NBR index, originally developed to evaluate fire severity, is highly effective in detecting burned areas and tracking vegetation regeneration patterns across different post-fire phases (Veraverbeke, Hook, and Hulley 2012). NDWI and MNDWI were integrated to enhance the detection of water-related vegetation stress. NDWI improves the identification of vegetation water content and aquatic features (McFeeters 1996), while MNDWI increases water body separation in complex terrains (GUERAIDIA et al. n.d.).

The Normalized Multi-band Drought Index (NMDI) is utilized to capture both soil and vegetation moisture status, as it reflects combined surface and canopy water content and offers enhanced drought detection capabilities (Wang and Qu 2007). Similarly, SAVI and its extended form SAVI2 account for soil background effects; these were calculated using L=0.5 and L=1, respectively, to adapt to varying vegetation densities (Huete 1988; Wang and Qu 2007). Thermal variations due to fire-induced changes are assessed using Land Surface Temperature (LST), extracted from both daytime and nighttime data to reflect diurnal differences. LST plays a key role in regulating surface energy balance, evapotranspiration, and post-fire vegetation regrowth (Kustas and Anderson 2009; Vlassova et al. 2014).

Evapotranspiration (ET), the Evapotranspiration Deficit Index (ETDI), and various drought indices (including the Standardized Precipitation Evapotranspiration Index (SPEI) and the Standardized Precipitation Index (SPI)) are incorporated to account for complex hydroclimatic forcing. Furthermore, auxiliary ERA5-Land meteorological and hydroclimatic variables—such as total precipitation sum, air temperature, soil moisture, and relative humidity—are integrated to characterize the broader environmental conditions influencing post-fire vegetation recovery. These variables provide critical insights into vegetation resilience by explicitly representing moisture availability, atmospheric demand, and regional water balance conditions. The inclusion of this comprehensive feature set significantly enhances the predictive power of the MLP model, enabling a robust spatiotemporal analysis of vegetation regrowth, degradation, and long-term ecosystem transitions following fire disturbances. A detailed overview of all RS and meteorological indices utilized in this study is presented in Table 2.

Table 2. Characteristics of the studied wildfires in the United States and Spain.

Index	Definition	Formula	Resolution	Source
NDVI	Normalized Difference Vegetation Index	$\frac{NIR - RED}{NIR + RED}$	500 m, 8 Days	MOD09A1
NBR	Normalized Burn Ratio	$\frac{NIR - SWIR1}{NIR + SWIR1}$		
NDWI	Modified Normalized Difference Water Index	$\frac{Green - NIR}{Green + NIR}$		
NMDI	Normalized Multi-band Drought Index	$\frac{NIR - (SWIR1 - SWIR2)}{NIR + (SWIR1 - SWIR2)}$		
MNDWI	Modified Normalized Difference Water Index	$\frac{Green - SWIR1}{Green + SWIR1}$		
EVI	Enhanced Vegetation Index	$2.5 \times \frac{NIR - RED}{NIR + 6 \times RED - 7.5 \times Blue + 1}$		
EVI2	Enhanced Vegetation Index2	$2.5 \times \frac{NIR - RED}{NIR + 2.4 \times RED + 1}$		
SAVI	Soil Adjusted Vegetation Index	$1.5 \times \frac{NIR - RED}{NIR + RED + 0.5}$		
SAVI2	Soil Adjusted Vegetation Index2	$2 \times \frac{NIR - RED}{NIR + RED + 1}$		

LST Day	Land Surface Temperature	-	1km, Daily	MOD11A1
LST Night		-		
ET	Evapotranspiration	-	500 m, 8 Days	MOD16A2
ETDI	Evapotranspiration Deficit Index	$\frac{PET - ET}{PET}$	5566 m, Daily	MOD16A2 CHIRPS
PCI	Precipitation Concentration Index	$\frac{\sum P_i^2}{(\sum P_i)^2}$	1km, 8 Days 5566 m, Daily	CHIRPS
SPEI	Standardized Precipitation Evapotranspiration Index	$PET = 7.5 \times ET$ $\frac{\text{Precipitation - PET}}{\text{PET}}$	5566 m, Daily	MOD16A2 CHIRPS
SPI	Standardized Precipitation Index	$\frac{StdPrecipitation - Mean}{Std}$	11132 m, Monthly Averaged	CHIRPS
Temperature	Air Temperature at 2m: Atmospheric temperature at 2 meters above the surface	-	11132 m, Monthly Averaged	ERA5-Land
Precipitation	Total Precipitation Sum: Total accumulated precipitation over a period	-		
Soil Moisture	Volumetric Soil Water Content (0-7cm layer): Amount of water present in the top layer of soil	-		

3. Methods

This study employs a robust methodology that integrates multi-source RS data, MLP model techniques, and specific recovery metrics to comprehensively assess post-fire vegetation dynamics across diverse fire-affected regions. The methodological framework is designed to overcome limitations inherent in traditional approaches by leveraging the power of cloud-based platforms and deep learning, thereby enabling the capture of complex, non-linear recovery patterns. The overall process, spanning data acquisition, preprocessing, model training, and performance evaluation, is illustrated in Figure 2 and detailed in the following subsections.

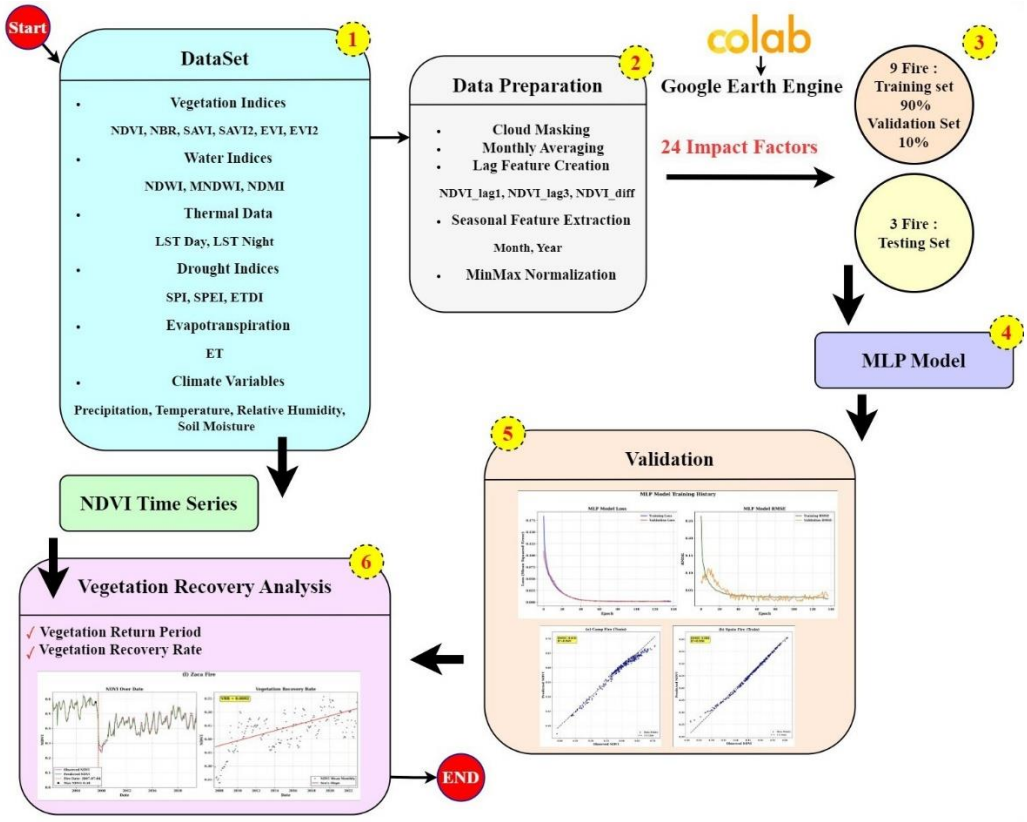

Figure 2. Methodology for Assessing Post-Fire Vegetation Dynamics using MLP and RS.

3.1. Data Preparation

The foundation of this study relies on an extensive collection of RS and environmental data spanning from January 2000 to December 2022, all processed and managed within the GEE platform. GEE's capabilities were instrumental in accessing and processing large volumes of satellite imagery and meteorological datasets, thus ensuring efficient handling of spatiotemporal data for the twelve selected wildfire events in the United States and Spain. All time series data were aggregated to monthly averages to capture seasonal and inter-annual variations. For consistency and computational feasibility, averaged NDVI values across each fire perimeter were used to generate a representative recovery trajectory. This spatial averaging methodology facilitated the comparison of dynamics across 12 extensive, multi-regional wildfire events spanning more than two decades. Furthermore, to account for temporal dependencies and seasonal indicators, features such as NDVI lag1 (previous month's NDVI), NDVI lag3 (NDVI from three months prior), and NDVI diff (difference from previous month's NDVI) were engineered. The month and year of each observation were also explicitly included as seasonal features. All input features were subjected to MinMaxScaler normalization and scaled according to the target parameter (NDVI), which ensures numerical stability during training and prevents features with larger values from dominating the learning process. This comprehensive feature set allowed for a nuanced understanding of the complex interactions influencing post-fire vegetation recovery.

3.2. MLP Model Architecture and Training

Neural networks constitute a class of algorithms utilized for either classification or function approximation (RP 1987).). Among the various types, the Multi-Layer Perceptron (MLP) is the most commonly employed Artificial Neural Network (ANN). MLPs are specifically designed to model complex, nonlinear relationships between input and output variables, excelling at processing vast datasets and uncovering latent patterns. The integration of RS data with MLP algorithms facilitates a more comprehensive analysis, as these models effectively leverage the rich temporal and spatial information captured by satellite platforms (Eaturu and Vadrevu 2025).

An MLP architecture comprises an input layer, one or more hidden layers, and an output layer. Each layer is composed of neurons that process information by applying weights and biases to the inputs (Eaturu and Vadrevu 2025). In operation, data samples are typically fed into the input layer following normalization. The input data is then propagated through the hidden layers, where neurons compute weighted sums of their inputs and apply an activation function. This iterative process continues through

subsequent layers until the final output layer yields the model's prediction. The optimal choice of the number of hidden layers and nodes per layer remains an open research question, although several heuristics exist, some developed specifically for RS (e.g., the Kanellopoulos–Wilkinson (1997) rule) (Stathakis and Vasilakos 2006). A key advantage of neural networks is their capacity to incorporate multiple data sources, including non-spectral data, as inputs (Benediktsson, Swain, and Ersoy 1990; Stathakis and Kanellopoulos 2008), given that they make no assumptions about the statistical distributions of the input data.

In this study, the MLP model architecture specifically comprised an input layer connected to a hidden layer with 128 neurons, followed by a second hidden layer containing 64 neurons, and concluded with an output layer consisting of a single neuron dedicated to continuous NDVI prediction. The Rectified Linear Unit (ReLU) activation function was consistently applied to the hidden layers. To ensure robust generalization and effectively prevent overfitting, the model incorporated several key regularization techniques. L2 Regularization, with a factor of 0.001, was applied to the weights of the dense layers; this technique functions by adding a penalty to the loss function proportional to the square of the weights' magnitude, thereby discouraging overly large weights and promoting simpler, more generalizable models. Furthermore, Dropout Layers were implemented with a dropout rate of 0.5, applied specifically after the first dense layer. Dropout operates by randomly setting a fraction of input units to zero during each training update, a mechanism that helps prevent the co-adaptation of neurons and significantly enhances the model's capacity to generalize effectively to previously unseen data.

The training process was meticulously structured, adhering to a three-set strategy for objective validation (Bishop 1995). For each of the nine fire events designated for training, 90% of its respective data was allocated for training, and the remaining 10% was reserved for validation. These individual subsets were subsequently aggregated to form the comprehensive training and validation sets. This approach ensured that the model's performance was monitored on unseen data from each fire before aggregation. Crucially, three entirely independent fire events—namely, the Thomas Fire, King Fire, and Zaca Fire—were designated as a separate testing set, a critical component for rigorously evaluating the model's generalization capability on completely novel data. The model's optimization was achieved using the Adam optimizer, commencing with an initial learning rate set at 0.0005. Training was systematically conducted for 200 epochs, utilizing a batch size of 32 for each iteration. To further enhance training stability and diligently prevent overfitting, several callbacks were implemented. The EarlyStopping callback, configured with a patience of 30, continuously monitored the validation loss; training was automatically halted if no improvement was observed for 30 consecutive epochs, thereby precluding model overtraining. Additionally, the ReduceLROnPlateau callback, with a patience of 25, similarly monitored the validation loss; should the validation loss fail to improve for 25 consecutive epochs, the learning rate was automatically reduced by a predefined factor. The comprehensive set of hyperparameters employed for the MLP model is concisely summarized in Table 3.

Table 3. Hyperparameters and Callbacks of the MLP Model.

Hyperparameter	Value
Epochs	200
Batch Size	32
Learning Rate	0.0005
Optimizer	Adam
Model Architecture	Dense (128) → Dropout (0.5) → Dense (64)
Dropout Rate	0.5
L2 Regularization	0.001
Callbacks	Early Stopping (patience=30), ReduceLROnPlateau (patience=25)

3.2.1. Extension and Novelty of the MLP Framework

While the Multi-Layer Perceptron (MLP) architecture described in Section 3.2 is a well-established deep learning model, this study significantly advances its application for post-fire vegetation recovery analysis through three major extensions. These advancements collectively address the critical limitations inherent in earlier index-based and linear modeling approaches:

(i) Comprehensive Feature Integration (Technical Extension): The proposed framework moves beyond traditional spectral inputs (e.g., NDVI and NBR) by integrating a comprehensive suite of multi-source predictors, including vegetation, hydrological, thermal (LST and ET), and climatic/drought-related indices. This enriched feature space enables the MLP to capture the inherently non-linear dependencies among vegetation recovery, fire severity, and climate drivers—complex relationships that standard linear regression or single-index methods cannot effectively represent.

(ii) Temporal Dependence Encoding: Temporal memory and seasonal variation are explicitly encoded into the model through engineered lagged features (NDVI lag1, NDVI lag3) and differenced variables (NDVI diff). These inputs encode sequential context within the static feed-forward network, allowing the MLP to infer vegetation dynamics based on past conditions. This modification effectively adapts the conventional MLP framework to time-series forecasting without requiring more complex recurrent or convolutional architectures.

(iii) Rigorous Generalization Testing (Methodological Extension): Model robustness and transferability were assessed through rigorous testing on three geographically and temporally independent wildfire events—specifically, the Thomas, King, and Zaca Fires. These events were completely excluded from the model training and validation processes. This rigorous design allows for an unbiased evaluation of how well the trained MLP generalizes to completely unseen ecosystems and climatic regimes,

thereby demonstrating its potential for scalable, operational remote-sensing applications.

Together, these extensions establish a robust and transferable deep-learning framework uniquely capable of modeling the spatiotemporal complexity of post-fire vegetation resilience across diverse global environments.

3.3. Performance Evaluation and Recovery Metric

The performance of the MLP model was evaluated through rigorous testing on the three independent fire events (Thomas Fire, King Fire, and Zaca Fire) to assess the model's ability to generalize to completely unseen data. Post-fire vegetation recovery was quantitatively assessed using two key metrics: Sen's Slope (referred to as the Vegetation Recovery Rate – VRR) and the Vegetation Recovery Period (VRP).

Sen's Slope, a non-parametric method, was employed for trend analysis of the observed NDVI time series, thereby quantifying the annual rate of NDVI change. A positive slope indicates vegetation greening (recovery), while a negative slope suggests browning (degradation). The VRP measured the time required for the observed NDVI to recover to a certain percentage of its pre-fire baseline. The pre-fire baseline NDVI was specifically defined as the maximum NDVI value observed within the one year preceding the fire event. VRP was calculated at three distinct thresholds: 50%, 70%, and 90% of this pre-fire baseline NDVI, providing a nuanced understanding of recovery speed and resilience across various stages of ecological succession.

In addition to their mathematical definition, these VRP thresholds correspond to ecologically meaningful stages of recovery. VRP 50% generally reflects early regrowth dominated by herbaceous or shrub cover, contributing to soil stabilization. VRP 70% indicates intermediate recovery, where partial canopy closure begins to restore habitat quality and microclimatic conditions. VRP 90% represents advanced recovery, where canopy structure and ecological processes, such as biomass accumulation and carbon uptake, approach pre-fire conditions. These metrics, combined with the comprehensive input features and the robust MLP framework, allowed for a detailed spatiotemporal analysis of post-fire vegetation recovery, degradation, and long-term ecosystem transitions, focusing on the actual observed trends.

4. Result

This section presents the core findings of the study, encompassing both the performance evaluation of the developed MLP model and the quantitative assessment of post-fire vegetation recovery dynamics. The predictive capability of the trained MLP model is first evaluated using multiple statistical performance metrics and a visual comparison between observed and predicted NDVI values. Subsequently, the derived vegetation recovery indicators—VRR and VRP—are examined across the selected wildfire events to highlight regional differences and temporal trends in recovery trajectories.

4.1. Post-Fire Vegetation Recovery Dynamics

The predictive capability of the Multi-Layer Perceptron (MLP) model was rigorously evaluated through both internal (training/validation) and external (test) assessments. The model was trained on nine wildfire events and tested on three independent fire events (Thomas, King, and Zaca Fires) to assess its generalization capacity on entirely unseen data. Performance was quantified using the Root Mean Squared Error (RMSE) and the coefficient of determination (R^2), which are standard metrics for evaluating regression models in remote sensing and ecological forecasting tasks.

Figure 3 presents scatter plots comparing the observed NDVI values with the MLP-predicted NDVI values for all twelve fire events. The close alignment of data points along the dashed 1:1 line indicates high model accuracy and strong agreement between predicted and actual values, with minimal deviation across both training and test sites. This consistency demonstrates the model's capacity to effectively capture the non-linear and region-specific dynamics of post-fire vegetation recovery, even within ecologically diverse areas.

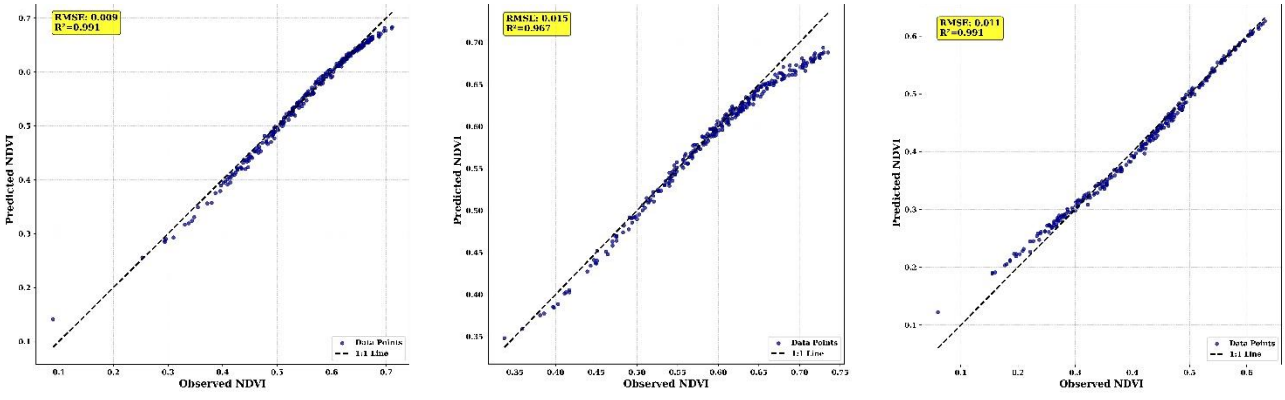

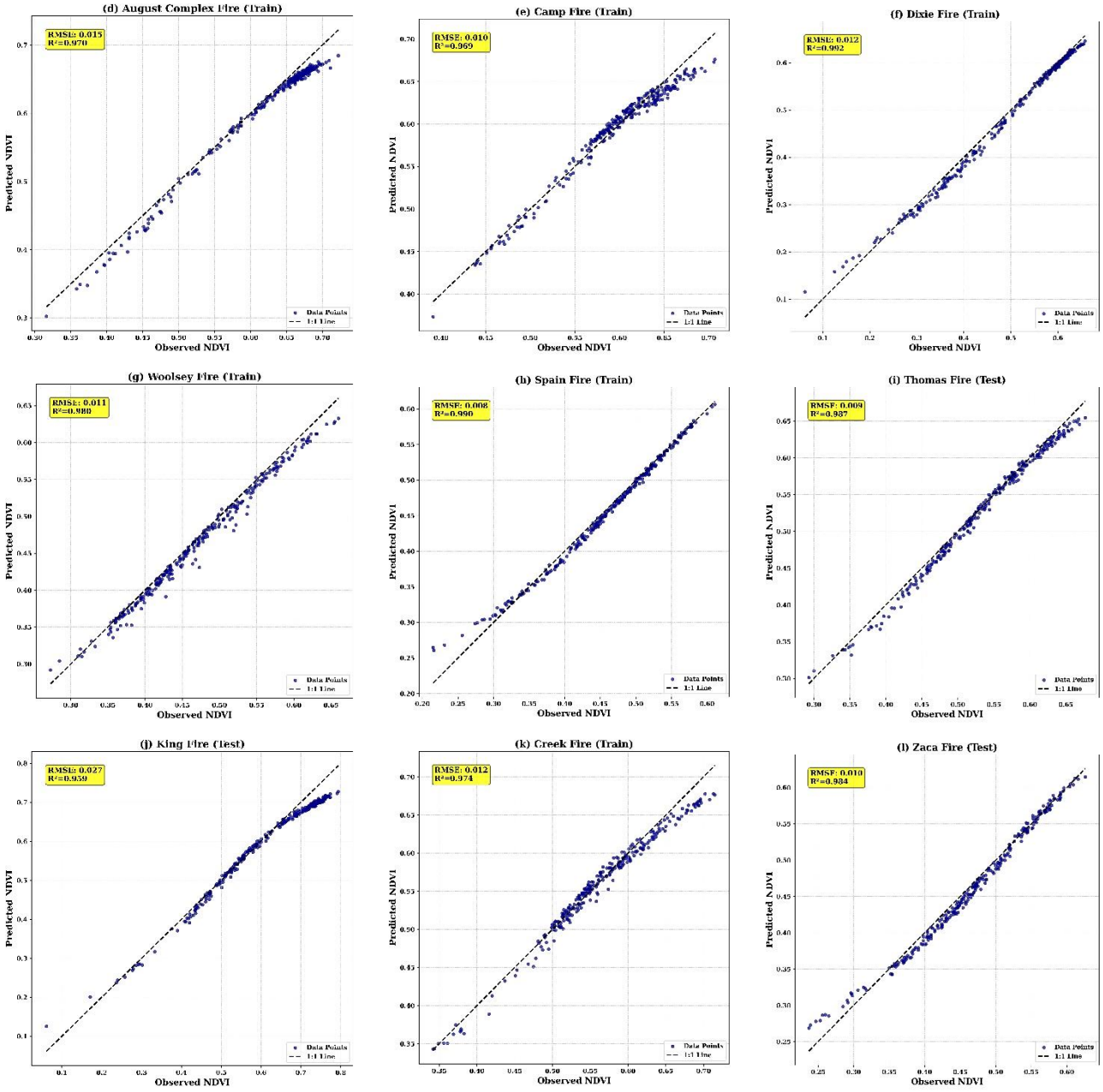

Figure 3. Scatter plots illustrating the relationship between observed and MLP-predicted NDVI values for: (a) Rim Fire, (b) Bastrop County Fire, (c) Waldo Canyon Fire, (d) August Complex Fire, (e) Camp Fire, (f) Dixie Fire, (g) Woolsey Fire, (h) Spain Fire, (i) Thomas Fire, (j) King Fire, (k) Creek Fire, and (l) Zaca Fire. The dashed black line represents the 1:1 line, indicating perfect agreement between predicted and observed values.

The detailed performance metrics are provided in Table 4, showing R^2 values exceeding 0.95 across all sites, and RMSE values generally below 0.015 for the training regions. Among the training fires, the Dixie Fire (R^2 = 0.992, RMSE = 0.012) and Rim Fire (R^2 = 0.991, RMSE = 0.009) demonstrated particularly strong results. Importantly, the MLP model also maintained robust performance on the independent test fires. The Thomas Fire achieved R^2 = 0.987 and RMSE = 0.009, indicating near-perfect agreement with observed values. Similarly, the Zaca Fire showed strong generalization with R^2 = 0.984 and RMSE = 0.010. While the King Fire, which was characterized by higher post-fire NDVI fluctuations, exhibited slightly lower performance (R^2 = 0.959, RMSE = 0.027), the result remains strong, validating the model's robustness across complex recovery trajectories.

Beyond the numerical performance metrics, the variation in R^2 and RMSE values across the twelve fire sites directly reflects underlying ecological complexity, landscape heterogeneity, and climatic regimes. Sites characterized by comparatively higher RMSE values, such as the Dixie and King Fires, are often subject to more pronounced seasonal NDVI fluctuations and stronger inter-annual climate variability. These dynamic environmental conditions present a greater challenge for precise predictive modeling. Conversely, sites like the Rim and Zaca Fires exhibited smoother and more stable NDVI trajectories post-disturbance, correlating with lower prediction errors. This contrast suggests that the MLP model achieves its highest predictive accuracy in regions with relatively consistent vegetation phenology and predictable seasonal cycles. Crucially, the model is demonstrated to maintain robust performance even under the challenging conditions of climatically dynamic or highly heterogeneous ecosystems. This qualitative interpretation underscores the MLP's ability to successfully generalize across diverse ecological contexts while simultaneously capturing site-specific recovery dynamics with high fidelity.

Table 4. Performance Metrics (RMSE and R^2) of the MLP Model on Comprehensive Training, Validation, and Independent Test Datasets.

Fire Dataset	R-Squared	RMSE
Rim	0.991	0.009
Bastrop County	0.969	0.015
Waldo Canyon	0.991	0.011
August Complex	0.970	0.015
Camp	0.969	0.010
Dixie	0.992	0.012
Woolsey	0.980	0.011
Spain	0.990	0.008
Thomas	0.987	0.009
King	0.959	0.027
Creek	0.974	0.012
Zaca	0.984	0.010

Figure 4 presents the training history of the MLP model over 140 epochs, showing the convergence patterns for both the Mean Squared Error (MSE) loss and RMSE. Figure 4a displays a consistent decline in both the training and validation loss curves, which reached a plateau after approximately 80 epochs, indicative of good convergence without overfitting. Figure 4b confirms that RMSE remained stable and comparable for both the training and validation sets across epochs. The successful application of regularization techniques (L2 and dropout), combined with EarlyStopping and learning rate reduction callbacks, effectively mitigated overfitting and enhanced model generalization.

These results collectively validate the MLP model's robustness in accurately modeling complex, non-linear vegetation recovery trajectories using a diverse set of biophysical and climatic predictors. The strong performance observed on both training and independent test sites underscores the framework's applicability for large-scale and transferable post-fire recovery assessments.

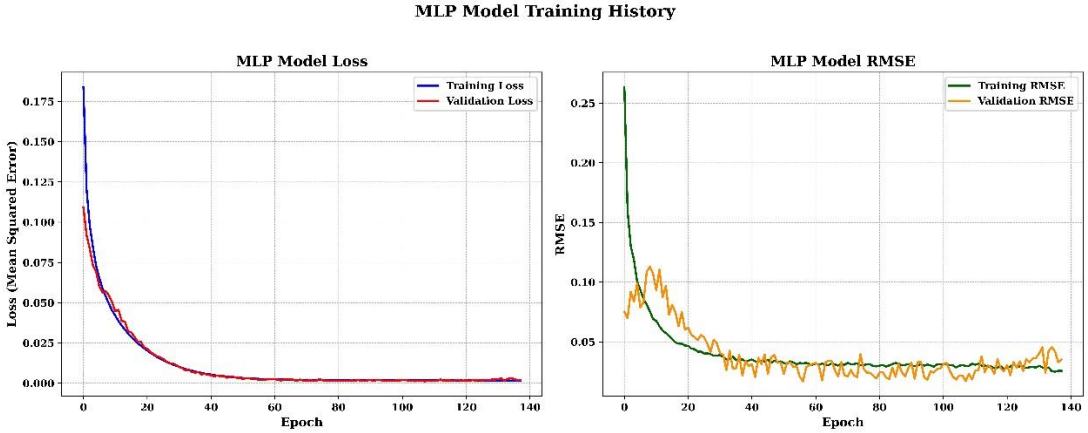

Figure 4. Training history of the MLP model. (a) Mean Squared Error (MSE) loss for the training and validation datasets over 140 epochs. (b) Root Mean Squared Error (RMSE) for the training and validation datasets.

4.2. Post-Fire Vegetation Recovery Dynamics

This subsection presents a comprehensive analysis of post-fire vegetation recovery across the twelve studied wildfire events1, utilizing two key indicators derived from the observed NDVI time series: the Vegetation Recovery Rate (VRR), quantified via Sen's Slope, and the Vegetation Recovery Period (VRP) at 50%, 70%, and 90% thresholds of the pre-fire NDVI baselines. Figure 4 visually illustrates the observed and MLP-predicted NDVI time series, coupled with the calculated Sen's Slope trends for each fire event. A detailed summary of these recovery metrics is provided in Table 5.

The analysis revealed that the majority of the wildfire sites exhibited positive recovery trends, with a VRR greater

than zero, signifying progressive greening and vegetation regeneration following the disturbance. Notable exceptions, however, were the Dixie Fire and Woolsey Fire, which displayed negative VRR values of −0.009 and −0.005, respectively. These negative trends suggest a sustained decline in NDVI post-fire, indicating potential long-term degradation. This sustained decline could be attributed to compounding factors such as exceptionally severe fire intensity, prolonged drought stress, or inhibited natural regeneration processes specific to these ecosystems.

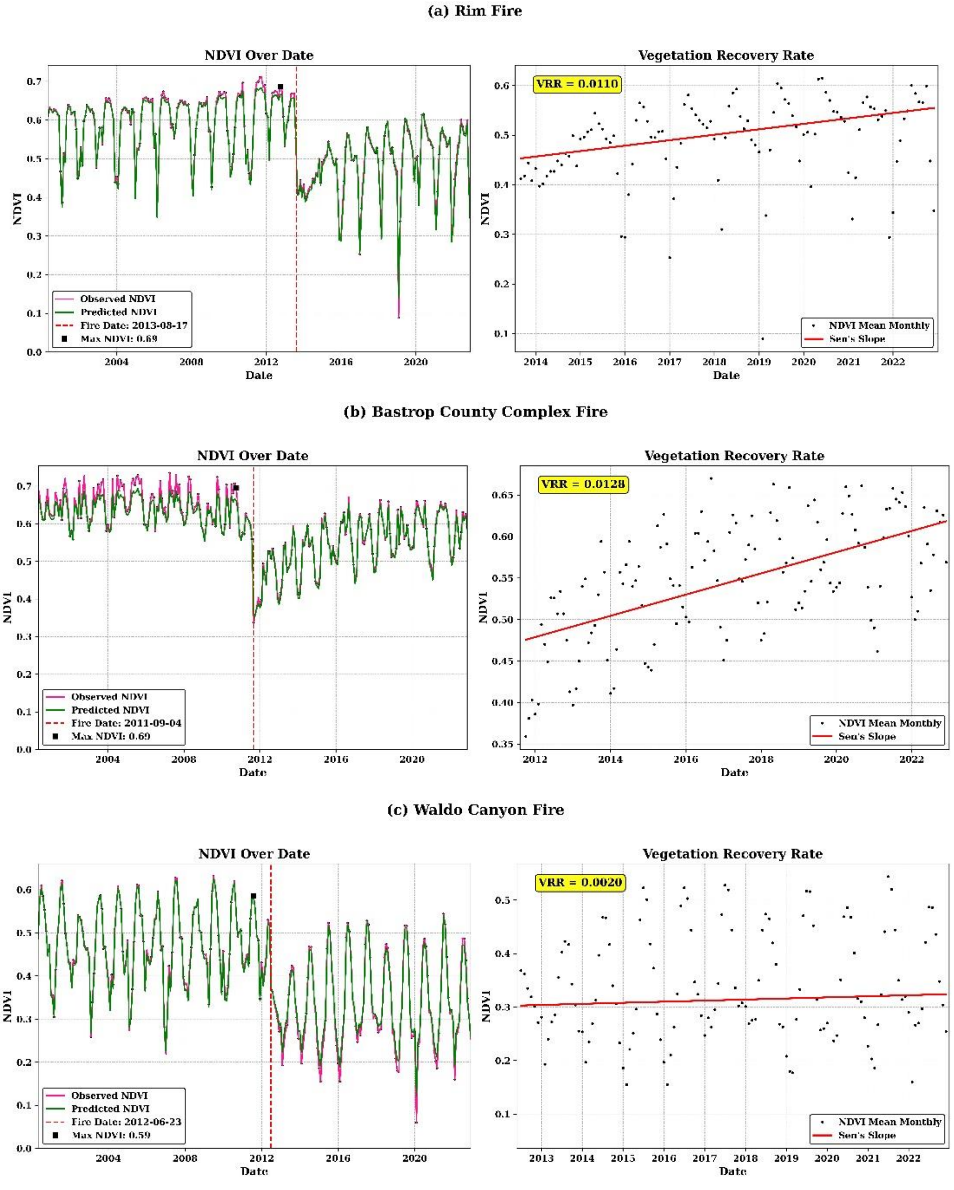

(d) August Complex Fire

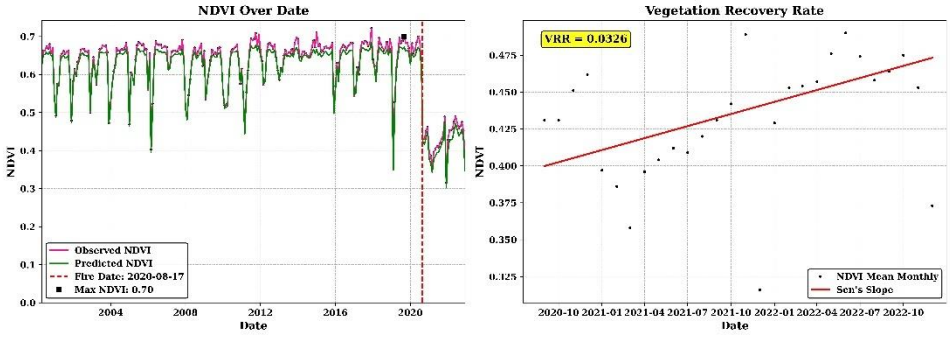

(e) Camp Fire

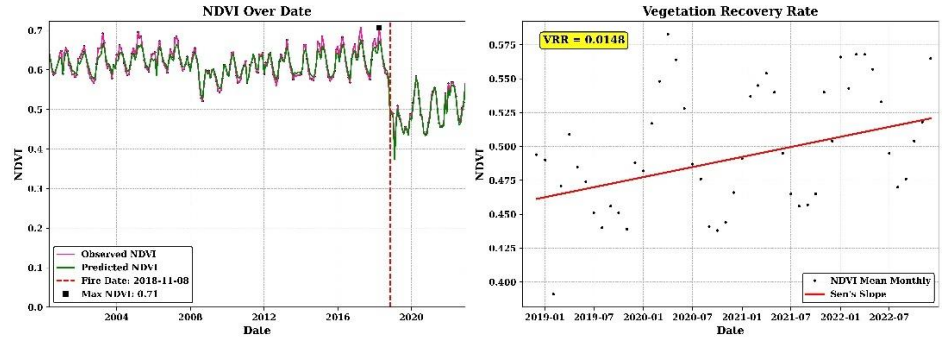

(f) Dixie Fire

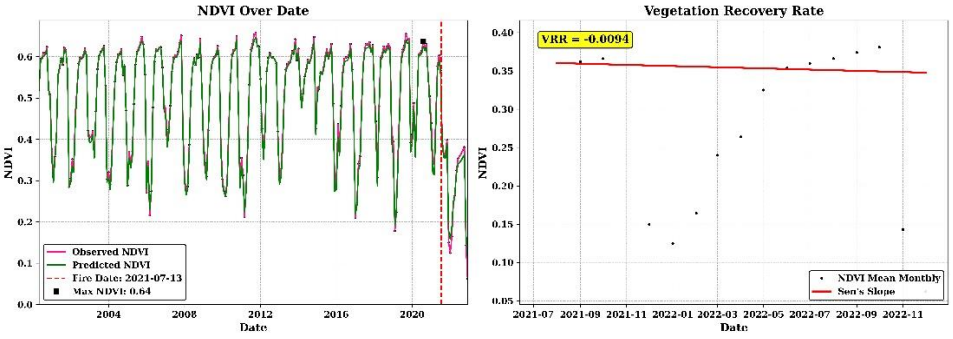

(g) Woolsey Fire

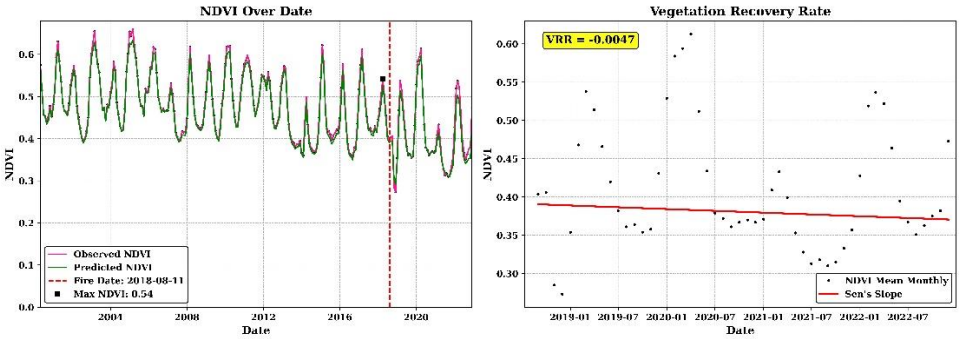

(h) Spain Fire

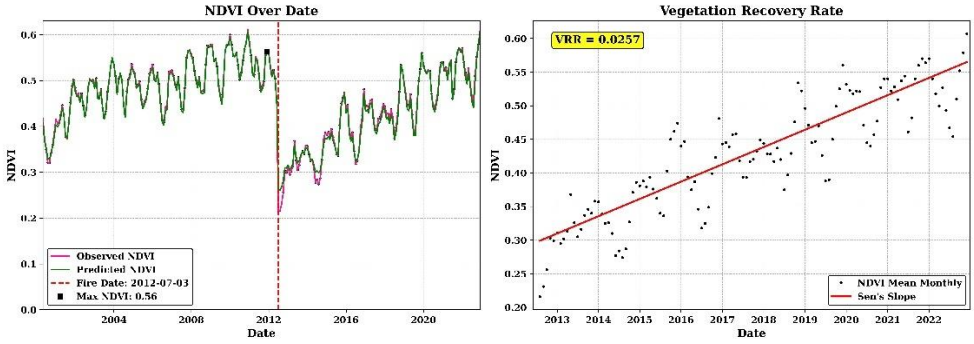

(i) Thomas Fire

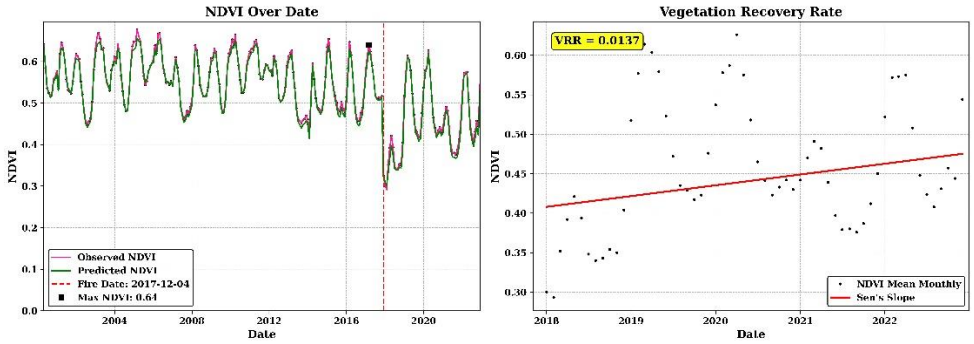

(j) King Fire

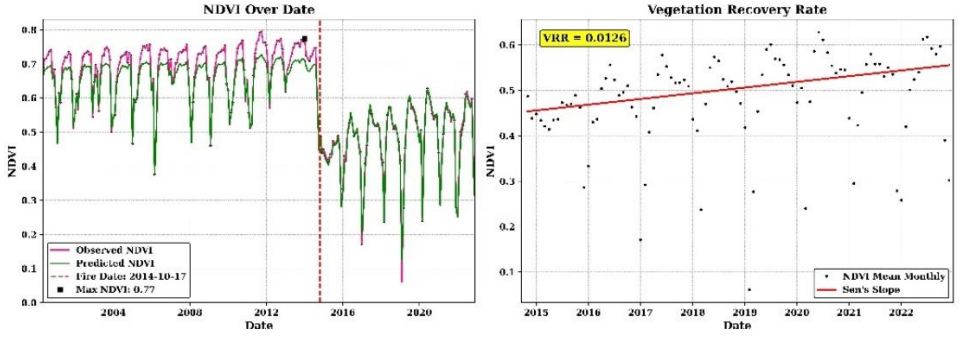

(k) Creek Fire

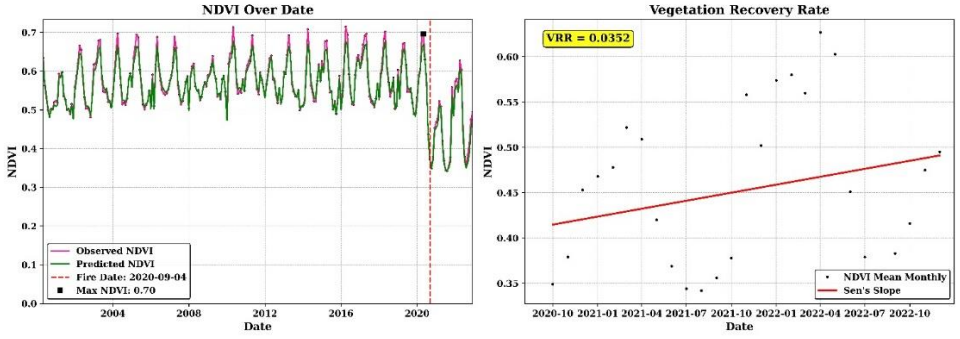

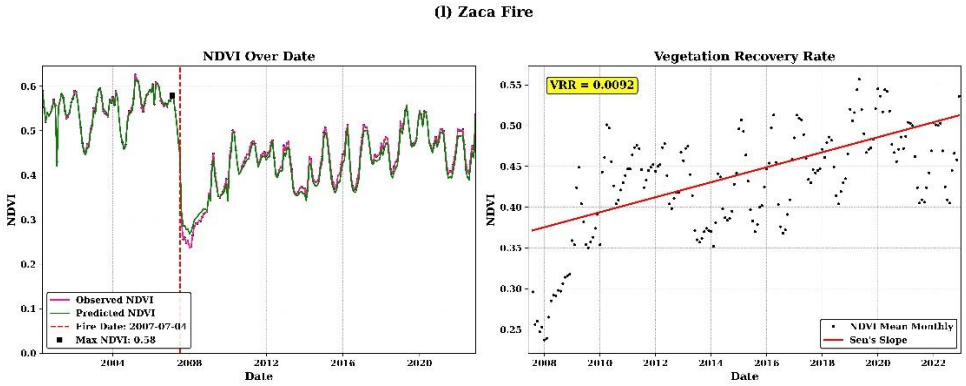

Figure 4. Monthly time series of observed and MLP-predicted NDVI values and vegetation recovery trends for twelve wildfire events. Each panel presents (left) the time series of observed (pink line with black circles) and predicted (green line with green squares) NDVI, with the fire date marked by a vertical dashed red line. The right side of each panel shows the linear Sen's slope regression (red line) fitted to the observed monthly NDVI values post-fire. The calculated Vegetation Recovery Rate (VRR) is displayed in yellow boxes.

Conversely, the August Complex Fire and Creek Fire demonstrated the most vigorous and rapid recovery trajectories among the studied events, characterized by the highest VRR values of 0.032 and 0.035, respectively. For both these fires, the observed NDVI values rebounded swiftly, reaching 70% of their pre-fire baseline within approximately 7–14 months. Nevertheless, neither fire achieved 90% recovery within the defined study period, which implies robust initial regrowth and re-establishment of ground cover but potentially a more protracted process for full canopy closure or complete ecosystem restoration.

In contrast to the rapid recovery sites, the Zaca Fire exhibited the longest VRP90 among all analyzed sites, spanning 4287 days (approximately 11.7 years). This extended recovery occurred despite a positive VRR of 0.009, highlighting a protracted and gradual recovery process characteristic of its Mediterranean shrubland ecosystem. Similarly, the Spain Fire required 2313 days (approximately 6.3 years) to attain 90% of its NDVI baseline, a slower recovery likely influenced by the prevailing climatic constraints and inherently lower vegetation productivity typical of its semi-arid environment.

Fires such as the Bastrop County Complex, Thomas, Waldo Canyon, and Camp Fires exhibited moderate to high VRR values, ranging from 0.013 to 0.015, and successfully reached VRP90 within 3.5 to 5 years. This consistent pattern indicates a stable rate of regrowth in these primarily forested regions. It is particularly noteworthy that the Thomas Fire, which was utilized as an independent test fire for the MLP model, showed recovery patterns that aligned well with general observed trends, reinforcing the model's overall generalization capability.

Furthermore, sites including the Rim, King, and Waldo Canyon Fires achieved 50% and 70% NDVI thresholds within approximately one year post-fire, suggesting high initial vegetation resilience. However, the Waldo Canyon Fire displayed a relatively low VRR (0.002), indicating a slow rate of greening despite reaching earlier recovery milestones. This discrepancy could be a result of high seasonal NDVI fluctuations or specific post-fire environmental conditions. As depicted in Figure 4, the MLP-predicted NDVI values closely followed the observed NDVI trends across all fire events, effectively capturing seasonal variations and approximating the long-term recovery patterns. The model accurately identified sharp NDVI drops immediately following fire dates and was able to predict the subsequent upward trends with high fidelity, demonstrating consistency with the overall model performance presented in Figure 3 and Table 4.

Table 5. Post-fire vegetation recovery metrics across the twelve wildfire events. This table includes the pre-fire baseline NDVI values, the Vegetation Recovery Period (VRP) measured as the time (in days) required to reach 50%, 70%, and 90% of the pre-fire baseline NDVI, the calculated Vegetation Recovery Rate (VRR), and the final classification of recovery status (Greening or Browning) based on the VRR.

Fire Name	BASE NDVI	VRP 50%	VRP 70%	VRP 90%	RR	Recovery Status
Rim	0.687	380	440	-	0.011	Greening
Bastrop County Complex	0.695	393	393	1369	0.013	Greening
Waldo Canyon	0.586	374	404	1838	0.002	Greening
August Complex	0.7	382	653	-	0.032	Greening
Camp	0.706	389	449	-	0.015	Greening
Dixie	0.637	385	-	-	-0.009	Browning
Woolsey	0.542	388	477	509	-0.005	Browning
Spain	0.563	395	1155	2313	0.026	Greening
Thomas	0.64	393	393	424	0.014	Greening
King	0.774	380	593	-	0.013	Greening
Creek	0.696	392	422	573	0.035	Greening
Zaca	0.579	394	606	4287	0.009	Greening

A qualitative examination of Table 5 further reveals that faster recovery rates (high VRR, short VRP) are typically

associated with forested and temperate ecosystems, where adequate soil moisture and nutrient availability facilitate rapid post-fire regrowth. In sharp contrast, water-limited environments, specifically Mediterranean and semi-arid regions such as the Zaca and Spain Fires, consistently exhibit slow or incomplete recovery, a pattern consistent with limited regeneration potential and increased susceptibility to post-fire erosion. The negative VRR observed for sites like the Dixie and Woolsey Fires likely indicates the influence of compounding factors such as extreme burn severity, prolonged antecedent drought, or subsequent anthropogenic disturbances, highlighting the high sensitivity of these systems to climatic extremes. These regional and ecological contrasts reinforce the utility and ecological relevance of VRR and VRP as quantitative indicators of ecosystem resilience, effectively linking the modeled recovery trajectories to underlying biophysical and climatic constraints.

5. Discussion

This study presents a comprehensive assessment of post-fire vegetation recovery across twelve diverse wildfire events using a data-driven MLP model trained on multi-source remote sensing time series. The high performance of the model (with R^2 values>0.95 across all sites) affirms the efficacy of deep learning algorithms in capturing complex ecological processes such as fire-driven vegetation transitions, thereby surpassing the capability of traditional regression or single-index threshold approaches (Alonso-González and Fernández-García 2021; Cardil et al. 2021).

5.1. Interpreting Regional Recovery Patterns

The calculated Vegetation Recovery Rates (VRR) and Recovery Periods (VRP) reveal notable heterogeneity in post-fire vegetation responses across regions. Fires in forested temperate and humid ecosystems—such as the Creek, Camp, and Thomas Fires—showed relatively rapid recovery, reaching 90% of their pre-fire NDVI within approximately 2–5 years, supported by VRR values between 0.014 and 0.035. These trends align with previous studies demonstrating that coniferous and mixed forests often exhibit moderate to high resilience following fire, particularly when soil moisture and climatic conditions remain favorable post-disturbance (Bassett et al. 2017; Chen et al. 2010; Gilroy et al. 2014).

The qualitative analysis of Tables 4 and 5 underscores that both model accuracy and the resulting ecological recovery metrics are fundamentally governed by environmental context. High-performing sites are typically associated with ecosystems exhibiting rapid post-fire regrowth and stable climatic regimes. Conversely, lower-performing sites are concentrated in regions where vegetation is characterized by high temporal variability or sustained drought impacts. Consequently, the quantitative outputs not only affirm the model's statistical performance but also serve as a robust indicator of the inherent ecological variability present across diverse fire-prone landscapes.

The VRP thresholds (50%,70%,90%) correspond to distinct ecological stages of recovery, not merely arbitrary percentages. VRP 50% typically reflects the early re-establishment of ground cover, dominated by herbaceous or shrub species that contribute to soil stabilization and reduction of erosion risk. VRP 70% is generally associated with partial canopy recovery, where increased vegetation density begins to restore habitat quality and improve microclimatic conditions. VRP 90% indicates advanced successional stages, where canopy closure and biomass accumulation approach pre-fire conditions, thereby enhancing ecosystem services such as carbon sequestration, hydrological regulation, and habitat integrity (Arthur et al. 2012; Jeong, Ho, and Jeong 2009; Zou et al. 2020). By linking these thresholds to ecological processes, the VRP metrics provide not only temporal indicators of recovery but also insights into functional ecosystem resilience.

Conversely, Mediterranean and semi-arid environments—represented by the Zaca and Spain Fires—exhibited protracted recovery timelines. For instance, the Zaca Fire required nearly 12 years to return to the 90% NDVI baseline, despite recording a positive VRR (0.009). This observation aligns with previous studies (Viedma et al. 2015) and (San-Miguel-Ayanz et al. 2022), which reported that Mediterranean shrublands typically experience slower regeneration due to water stress, limited seedling recruitment, and increased post-fire erosion. Importantly, two sites—the Dixie and Woolsey Fires—exhibited negative VRR values, suggesting long-term vegetation degradation or stagnated regrowth. These findings may reflect the combined impacts of severe fire intensity, recurring drought, and potential land use changes, echoing the concerns raised by (Pausas and Keeley 2019) and (Anderegg et al. 2020) regarding increased fire vulnerability under climate change.

5.2. Recovery Trajectories with Fire Timing

By integrating fire start dates (Table 1) with VRP estimates, this study offers new insights into the temporal resilience of fire-affected ecosystems. The Rim and King Fires, for instance, achieved 50%–70% recovery within one year of burning, suggesting high early-stage resilience. Conversely, the Bastrop County Complex and Waldo Canyon Fires, despite eventually reaching 90% NDVI, required several years to attain intermediate thresholds. This delay may be indicative of differences in post-fire management strategies, fuel types, and climatic recovery support (Stevens et al. 2014). Such recovery timelines are valuable for fire ecology and policy, as they help identify the critical time windows during which active restoration, reseeding, or soil stabilization interventions might be most effectively applied. The long VRP90 observed in the Zaca and Spain Fires, for example, implies that these systems would benefit from prolonged

monitoring and potentially assisted recovery interventions.

5.3. Model Implications and Limitations

The strong alignment between MLP-predicted and observed NDVI time series highlights the model's ability to generalize across diverse spatial and climatic gradients. Unlike traditional linear models, the MLP effectively captured seasonal variations, internal dynamics, and abrupt shifts following fire events. This demonstrates the potential of neural networks for ecological forecasting, particularly when integrating multiple environmental variables (Karpatne et al. 2018; Reichstein et al. 2019).

Although this study did not perform an explicit model intercomparison with other machine learning algorithms, the achieved accuracy metrics ($R^2 > 0.95$; RMSE < 0.02) are competitive with, or demonstrably exceed, the performance reported in previous post-fire NDVI prediction studies using Random Forest or Gradient Boosting methods (e.g., (Alonso-González and Fernández-García 2021; Cardil et al. 2021)). These results strongly indicate that the MLP framework successfully captured complex, non-linear ecological dynamics inherent to vegetation recovery. Future research efforts are planned to include comprehensive comparative experiments with additional algorithms (e.g., Random Forest, XGBoost) to further quantify the relative advantages of the proposed deep learning approach.

Several limitations, however, merit consideration. First, NDVI, despite its effectiveness as a proxy for post-fire greenness, may underestimate structural recovery due to its well-documented saturation in dense canopies and sensitivity to soil background effects (Hao et al. 2022; Lopes et al. 2024). This inherent limitation underscores the importance of combining spectral and structural indicators. Structural datasets, such as GEDI-derived canopy height and aboveground biomass (Dubayah et al. 2020) or airborne LiDAR-based vegetation metrics (Toivonen et al. 2023), could offer a more nuanced representation of ecosystem recovery, particularly in dense forest settings where NDVI tends to saturate. Future research efforts should, therefore, aim to distinguish between rapid surface greening and true structural regeneration by integrating such complementary data sources.

A further limitation arises from the methodological decision to average NDVI across entire fire perimeters. While this approach ensured scalability and comparability across large and diverse fire events, it inevitably masks spatial heterogeneity. For instance, in very large fires such as the August Complex, recovery dynamics may vary substantially across burn severity gradients, vegetation types, or topographic conditions. Therefore, future research should consider stratified sampling (e.g., by severity classes or ecozones) or pixel-level analyses to better capture this fine-scale ecological variability.

Secondly, although the dataset spans 2000–2022, it primarily captures short- to mid-term recovery trajectories (up to approximately 15 years post-fire). This temporal scope risks overlooking critical long-term ecological processes, such as delayed tree mortality, successional species turnover, or complete ecosystem state shifts from forests to shrublands or grasslands (Pausas and Keeley 2019). Several studies suggest that recovery dynamics beyond 15–20 years can diverge substantially from early post-fire trends, particularly under conditions of recurrent droughts and climate change (Johnstone et al. 2016). Therefore, while the findings provide valuable insights into decadal-scale dynamics, caution is warranted when extrapolating them to longer-term ecosystem trajectories. Extended monitoring using forthcoming satellite missions and the integration of historical Landsat archives could assist in capturing these longer-term patterns in future research. A further limitation is the relatively small number of wildfire events, which constrains the generalizability of the findings. Expanding the training dataset to encompass a broader range of fire events across diverse ecosystems will be critical for improving the robustness and ensuring the transferability of the modeling framework.

Another important limitation is the absence of reported uncertainty estimates, including confidence intervals, sensitivity analyses, or error propagation. Although the findings provide valuable insights into recovery patterns, presenting them without explicit uncertainty measures may overstate their precision. Future research should therefore incorporate uncertainty quantification methods (e.g., bootstrapping, Monte Carlo simulations, or sensitivity analysis of predictor importance) to enhance the reliability of ecological interpretations.

In addition, some sites, such as the Dixie and Woolsey Fires, exhibited negative VRR values, reflecting a persistent decline in NDVI ('browning' trends) rather than recovery. These patterns may be driven by interacting ecological stressors, including prolonged drought conditions, invasive species encroachment, and increasing urban expansion into wildland–urban interface areas (Pausas and Keeley 2019; Stevens-Rumann et al. 2018). Such complex processes can suppress natural regeneration, favor type-conversion to shrublands or grasslands, and ultimately delay or prevent forest recovery. While the framework captures these trajectories, satellite greenness metrics alone cannot fully disentangle their underlying ecological drivers, underscoring the importance of combining spectral analyses with ecological field studies.

Lastly, the absence of in situ validation represents a key limitation. Although satellite-derived indices effectively capture broad post-fire trends, they cannot fully substitute for field-based ecological observations. Ground surveys of species composition, regeneration strategies, and biomass accumulation are critical to confirm whether spectral recovery corresponds to ecological recovery (Fernández-Guisuraga et al. 2021; Keeley, Beier, and Jenness 2021). Future studies should combine satellite data with field observations and ancillary structural datasets to improve ecological credibility and reduce uncertainty.

5.4. Management Relevance and Future Directions

From a management perspective, the lack of ground validation limits the immediate applicability of the results to site-specific restoration planning. In areas where negative VRR was observed (e.g., Dixie and Woolsey Fires), land managers should exercise caution in interpreting greenness recovery as definitive ecosystem resilience. These browning trends may indicate underlying ecosystem degradation linked to drought-induced mortality, invasive grass expansion, or urban pressures. Consequently, such regions may necessitate active interventions, such as reforestation, invasive species management, or soil moisture restoration, rather than relying solely on passive monitoring approaches. While the framework presented here successfully identifies broad patterns of post-fire recovery across regions, translating these outputs into actionable strategies requires integration with field-based evidence, including vegetation plots, species inventories, and post-fire biomass measurements.

The variability in VRR and VRP observed in this study emphasizes the need for fire-specific and regionally tailored recovery assessments. Areas exhibiting a prolonged VRP or negative VRR may require targeted restoration interventions (e.g., reseeding, invasive species control), whereas regions demonstrating rapid regrowth could be prioritized for passive recovery monitoring. In practical terms, the proposed framework offers direct support for post-fire management and climate adaptation planning. By quantitatively assessing both the VRR and VRP parameters of vegetation recovery, land managers can effectively identify areas at high risk of long-term degradation and strategically prioritize restoration or reforestation efforts. The model's demonstrated generalization capability across diverse fire-affected ecosystems positions it as an ideal tool for both early post-fire assessment and long-term monitoring at regional or national scales. Furthermore, the integration of multi-source remote sensing data enables scalable implementation within operational fire management systems, providing a robust decision-support tool for resource allocation, designing targeted recovery interventions, and evaluating the effectiveness of restoration programs under varying climatic conditions.

Moving forward, the incorporation of additional variables such as soil characteristics, fire severity maps (dNBR), land use patterns, and sociological factors could significantly enhance prediction accuracy and the robust classification of recovery pathways. Furthermore, management strategies should recognize that these results largely reflect decadal-scale recovery. Long-term trajectories extending beyond 15–20 years may reveal further ecological transitions, including shifts in dominant vegetation types or delayed mortality events, which were not fully captured within this temporal window. This highlights the importance of sustained monitoring programs and the incorporation of longer satellite archives to inform adaptive management under changing climate conditions. Moreover, embedding recovery thresholds into resilience frameworks could better inform adaptive management strategies under conditions of increasing fire frequency and climate variability (Jones et al. 2022; Rolnick et al. 2022).

6. Conclusion

This study successfully established a deep learning based MLP framework to rigorously assess post-fire vegetation recovery using multi-source remote sensing data. The model achieved high predictive accuracy ($R^2 > 0.95$ and RMSE < 0.02) and demonstrated robust transferability across diverse climatic and ecological regions. The strategic integration of vegetation, hydrological, and climatic indicators enabled the model to accurately capture non-linear recovery dynamics and to precisely quantify both VRR and VRP of post-fire regrowth. The results revealed distinct recovery trajectories among ecosystems. Forested temperate regions typically exhibited rapid and stable recovery (greening), whereas Mediterranean and semi-arid areas experienced slower recovery or even degradation trends, indicating potential long-term degradation risks. These findings fundamentally highlight the importance of site-specific monitoring and adaptive management to address ecosystem-specific recovery challenges. The VRR and VRP indicators thus serve as valuable, scalable tools for prioritizing active restoration efforts in high-risk regions over areas suitable for passive recovery monitoring.

Despite the strong predictive performance, several key limitations warrant acknowledgment. NDVI saturation and the absence of field-based structural data constrain the accurate interpretation of true biomass recovery. Furthermore, the relatively small number of wildfire events and the use of spatial averaging across fire perimeters may have obscured fine-scale ecological variability. Future research endeavors should focus on integrating LiDAR or GEDI-derived structural indicators, incorporating uncertainty quantification methods, and expanding the training dataset across different fire regimes to further enhance the robustness and transferability of the framework. In conclusion, this framework offers a practical and scalable solution for post-fire recovery monitoring and climate-informed land management. By providing ecologically interpretable and transferable indicators, it robustly supports operational decision-making for restoration prioritization, long-term resilience assessment, and adaptive management under the increasing pressures of wildfire activity and climate change.

Declaration of competing interest

The authors declare that they have no known competing financial interests or personal relationships that could have appeared to influence the work reported in this paper.

References

Abid, Faroudja. 2021. "A Survey of Machine Learning Algorithms Based Forest Fires Prediction and

Detection Systems." Fire Technology 57(2):559–90.
Alonso-González, Esteban, and Víctor Fernández-García. 2021. "MOSEV: A Global Burn Severity Database from MODIS (2000–2020)." Earth System Science Data 13(5):1925–38.
Al-Qthanin, Rahmah, and Rahaf Aseeri. 2025. "Assessment of Forest Fire Impact and Vegetation Recovery in the Ghalahmah Mountains, Saudi Arabia." Fire 8(5):172.
Anderegg, William R. L., Anna T. Trugman, Grayson Badgley, Christa M. Anderson, Ann Bartuska, Philippe Ciais, Danny Cullenward, Christopher B. Field, Jeremy Freeman, and Scott J. Goetz. 2020. "Climate-Driven Risks to the Climate Mitigation Potential of Forests." Science 368(6497):eaaz7005.
AnjanaDevi, V., P. Praveen, and R. Ramanathan. 2024. "Deep Learning for Wildfire Impact: Vegetation Recovery and Soil Chemistry Analysis." Pp. 762–68 in 2024 4th International Conference on Pervasive Computing and Social Networking (ICPCSN). IEEE.
Arthur, Anthony D., Peter C. Catling, and Allan Reid. 2012. "Relative Influence of Habitat Structure, Species Interactions and Rainfall on the Post-fire Population Dynamics of Ground-dwelling Vertebrates." Austral Ecology 37(8):958–70.
Ba, Rui, Michele Lovallo, Weiguo Song, Hui Zhang, and Luciano Telesca. 2022. "Multifractal Analysis of MODIS Aqua and Terra Satellite Time Series of Normalized Difference Vegetation Index and Enhanced Vegetation Index of Sites Affected by Wildfires." Entropy 24(12):1748.
Banskota, Asim, Nilam Kayastha, Michael J. Falkowski, Michael A. Wulder, Robert E. Froese, and Joanne C. White. 2014. "Forest Monitoring Using Landsat Time Series Data: A Review." Canadian Journal of Remote Sensing 40(5):362–84.
Bassett, Michelle, Steven W. J. Leonard, Evelyn K. Chia, Michael F. Clarke, and Andrew F. Bennett. 2017. "Interacting Effects of Fire Severity, Time since Fire and Topography on Vegetation Structure after Wildfire." Forest Ecology and Management 396:26–34.
Bastrop County Complex. 2012. "Texas A&M Forest Service. (2012, January 12). Nearly 1.5 Million Trees Expected to Die after Wildfire Ravages Bastrop County. Https://Tfsweb.Tamu.Edu/Nearly-1-5-Million-Trees-Expected-to-Die-after-Wildfire-Ravages-Bastrop-County/."
Bayoumi, Sahar, Khulood Alghamdi, Dalal Alqusair, and Abeer Alfutamani. 2018. "Visualization of Fire Accidents in Saudi Arabia." Pp. 1–6 in 2018 21st Saudi computer society national computer conference (NCC). IEEE.
Benediktsson, Jon A., Philip H. Swain, and Okan K. Ersoy. 1990. Neural Network Approaches versus Statistical Methods in Classification of Multisource Remote Sensing Data.
Bishop, Christopher M. 1995. Neural Networks for Pattern Recognition. Oxford university press.
CAL FIRE. 2007. "CAL FIRE. (2007). Zaca Fire Incident Report. California Department of Forestry and Fire Protection. Retrieved from Https://Www.Fire.ca.Gov/Incidents/2007/7/4/Zaca-Fire."
CAL FIRE. 2014. "CAL FIRE. (2014). King Fire Incident Report. California Department of Forestry and Fire Protection. Retrieved from Https://Www.Fire.ca.Gov/Incidents/2014/10/17/King-Fire."
CAL FIRE. 2017. "CAL FIRE. (2017). Thomas Fire Incident Report. California Department of Forestry and Fire Protection. Retrieved from Https://Www.Fire.ca.Gov/Incidents/2017/12/4/Thomas-Fire."
CAL FIRE. 2018a. "CAL FIRE. (2018). Camp Fire Incident Report. California Department of Forestry and Fire Protection. Retrieved from Https://Www.Fire.ca.Gov/Incidents/2018/11/8/Camp-Fire."
CAL FIRE. 2018b. "CAL FIRE. (2018). Woolsey Fire Incident Report. California Department of Forestry and Fire Protection. Retrieved from Https://Www.Fire.ca.Gov/Incidents/2018/11/8/Woolsey-Fire."
CAL FIRE. 2020a. "CAL FIRE. (2020). August Complex Fire Incident Report. California Department of Forestry and Fire Protection. Retrieved from Https://Www.Fire.ca.Gov/Incidents/2020/8/17/August-Complex-Includes-Doe-Fire."
CAL FIRE. 2020b. "CAL FIRE. (2020). Creek Fire Incident Report. California Department of Forestry and Fire Protection. Retrieved from Https://Www.Fire.ca.Gov/Incidents/2020/9/4/Creek-Fire."
CAL FIRE. 2021. "CAL FIRE. (2021). Dixie Fire Incident Report. California Department of Forestry and Fire Protection. Retrieved from Https://Www.Fire.ca.Gov/Incidents/2021/7/13/Dixie-Fire."
Cardil, Adrián, Santiago Monedero, Gavin Schag, Sergio de-Miguel, Mario Tapia, Cathelijne R. Stoof, Carlos A. Silva, Midhun Mohan, Alba Cardil, and Joaquin Ramirez. 2021. "Fire Behavior Modeling for Operational Decision-Making." Current Opinion in Environmental Science & Health 23:100291.
Carta, Francesco, Chiara Zidda, Martina Putzu, Daniele Loru, Matteo Anedda, and Daniele Giusto. 2023. "Advancements in Forest Fire Prevention: A Comprehensive Survey." Sensors 23(14):6635.
Chen, J. M., Ping Zhao, and X. Y. Guo. 2010. "Numerical Simulation of the Impact of Changes in the Vegetation in the Western China on the Summer Climate over the Northern China." Acta Meteor. Sinica 68(2):173–81.
Chuvieco, Emilio, Susana Martínez, María Victoria Román, Stijn Hantson, and M. Lucrecia Pettinari. 2014.

"Integration of Ecological and Socio-economic Factors to Assess Global Vulnerability to Wildfire." Global Ecology and Biogeography 23(2):245–58.

Chuvieco, Emilio, Florent Mouillot, Guido R. Van der Werf, Jesús San Miguel, Mihai Tanase, Nikos Koutsias, Mariano García, Marta Yebra, Marc Padilla, and Ioannis Gitas. 2019. "Historical Background and Current Developments for Mapping Burned Area from Satellite Earth Observation." Remote Sensing of Environment 225:45–64.

Davis, Kimberley T., Solomon Z. Dobrowski, Philip E. Higuera, Zachary A. Holden, Thomas T. Veblen, Monica T. Rother, Sean A. Parks, Anna Sala, and Marco P. Maneta. 2019. "Wildfires and Climate Change Push Low-Elevation Forests across a Critical Climate Threshold for Tree Regeneration." Proceedings of the National Academy of Sciences 116(13):6193–98.

Dubayah, Ralph, James Bryan Blair, Scott Goetz, Lola Fatoyinbo, Matthew Hansen, Sean Healey, Michelle Hofton, George Hurtt, James Kellner, and Scott Luthcke. 2020. "The Global Ecosystem Dynamics Investigation: High-Resolution Laser Ranging of the Earth's Forests and Topography." Science of Remote Sensing 1:100002.

Eaturu, Aditya, and Krishna Prasad Vadrevu. 2025. "Evaluation of Machine Learning and Deep Learning Algorithms for Fire Prediction in Southeast Asia." Scientific Reports 15(1):18807.

El-Rawy, Mustafa, Okke Batelaan, Nassir Al-Arifi, Ali Alotaibi, Fathy Abdalla, and Mohamed Elsayed Gabr. 2023. "Climate Change Impacts on Water Resources in Arid and Semi-Arid Regions: A Case Study in Saudi Arabia." Water 15(3):606.

Fernández-Guisuraga, José Manuel, Susana Suárez-Seoane, Paula García-Llamas, and Leonor Calvo. 2021. "Vegetation Structure Parameters Determine High Burn Severity Likelihood in Different Ecosystem Types: A Case Study in a Burned Mediterranean Landscape." Journal of Environmental Management 288:112462.

van Gerrevink, Max J., and Sander Veraverbeke. 2021. "Evaluating the Hyperspectral Sensitivity of the Differenced Normalized Burn Ratio for Assessing Fire Severity." Remote Sensing 13(22):4611.

Gilroy, James J., Paul Woodcock, Felicity A. Edwards, Charlotte Wheeler, Brigitte L. G. Baptiste, Claudia A. Medina Uribe, Torbjørn Haugaasen, and David P. Edwards. 2014a. "Cheap Carbon and Biodiversity Co-Benefits from Forest Regeneration in a Hotspot of Endemism." Nature Climate Change 4(6):503–7.

Gilroy, James J., Paul Woodcock, Felicity A. Edwards, Charlotte Wheeler, Brigitte L. G. Baptiste, Claudia A. Medina Uribe, Torbjørn Haugaasen, and David P. Edwards. 2014b. "Cheap Carbon and Biodiversity Co-Benefits from Forest Regeneration in a Hotspot of Endemism." Nature Climate Change 4(6):503–7.

Gimeno-García, Eugenia, Vicente Andreu, and José Luis Rubio. 2007. "Influence of Vegetation Recovery on Water Erosion at Short and Medium-Term after Experimental Fires in a Mediterranean Shrubland." Catena 69(2):150–60.

Girardin, Martin P. 2007. "Interannual to Decadal Changes in Area Burned in Canada from 1781 to 1982 and the Relationship to Northern Hemisphere Land Temperatures." Global Ecology and Biogeography 16(5):557–66.

Gorelick, Noel, Matt Hancher, Mike Dixon, Simon Ilyushchenko, David Thau, and Rebecca Moore. 2017. "Google Earth Engine: Planetary-Scale Geospatial Analysis for Everyone." Remote Sensing of Environment 202:18–27.

Goward, Samuel N., Compton J. Tucker, and Dennis G. Dye. 1985. "North American Vegetation Patterns Observed with the NOAA-7 Advanced Very High Resolution Radiometer." Vegetatio 64(1):3–14.

GUERAIDIA, NOUR E. L. HOUDA, SAIDA GUERAIDIA, RAMDANI RAYENE SIRINE, CHEMSEDDINE FEHDI, and HOUAM ABD EL KADER. n.d. "Natural Hazard Processing Analyze Investigation Using Different Spectral Indices (Ndvi, Ndwi, Mdwi, Savi, Ndbi, Nbr) Case Study of Souk Ahras Area North-Est of Algeria."

Hao, Bin, Xu Xu, Fei Wu, and Lei Tan. 2022. "Long-Term Effects of Fire Severity and Climatic Factors on Post-Forest-Fire Vegetation Recovery." Forests 13(6):883.

Hawe, R. G., and Donald M. Fuquay. 1969. "Remote Sensing of Lightning in Forest Fire Research." Remote Sensing of Environment, VI 1193.

He, Tingting, Jiwang Guo, Wu Xiao, Suchen Xu, and Hang Chen. 2023. "A Novel Method for Identification of Disturbance from Surface Coal Mining Using All Available Landsat Data in the GEE Platform." ISPRS Journal of Photogrammetry and Remote Sensing 205:17–33.

Helman, David, Itamar M. Lensky, Naama Tessler, and Yagil Osem. 2015. "A Phenology-Based Method for Monitoring Woody and Herbaceous Vegetation in Mediterranean Forests from NDVI Time Series." Remote Sensing 7(9):12314–35.

Hird, Jennifer N., Jahan Kariyeva, and Gregory J. McDermid. 2021. "Satellite Time Series and Google Earth Engine Democratize the Process of Forest-Recovery Monitoring over Large Areas." Remote Sensing 13(23):4745.

Huete, Alfredo, Kamel Didan, Tomoaki Miura, E. Patricia Rodriguez, Xiang Gao, and Laerte G. Ferreira. 2002. "Overview of the Radiometric and Biophysical Performance of the MODIS Vegetation Indices." Remote Sensing of Environment 83(1–2):195–213.

Huete, Alfredo R. 1988. "A Soil-Adjusted Vegetation Index (SAVI)." Remote Sensing of Environment 25(3):295–309.

Jeong, Su-Jong, Chang-Hoi Ho, and Jee-Hoon Jeong. 2009.

"Increase in Vegetation Greenness and Decrease in Springtime Warming over East Asia." Geophysical Research Letters 36(2).

Jeong, Su-Jong, Chang-Hoi Ho, Tae-Won Park, Jinwon Kim, and Samuel Levis. 2011. "Impact of Vegetation Feedback on the Temperature and Its Diurnal Range over the Northern Hemisphere during Summer in a 2× CO2 Climate." Climate Dynamics 37(3):821–33.

Jiang, Bo, and Shunlin Liang. 2013a. "Improved Vegetation Greenness Increases Summer Atmospheric Water Vapor over Northern China." Journal of Geophysical Research: Atmospheres 118(15):8129–39.

Jiang, Zhangyan, Alfredo R. Huete, Kamel Didan, and Tomoaki Miura. 2008. "Development of a Two-Band Enhanced Vegetation Index without a Blue Band." Remote Sensing of Environment 112(10):3833–45.

Joao, Torres, Gonçalves João, Marcos Bruno, and Honrado João. 2018. "Indicator-Based Assessment of Post-Fire Recovery Dynamics Using Satellite NDVI Time-Series." Ecological Indicators 89:199–212.

Johnstone, Jill F., Craig D. Allen, Jerry F. Franklin, Lee E. Frelich, Brian J. Harvey, Philip E. Higuera, Michelle C. Mack, Ross K. Meentemeyer, Margaret R. Metz, and George L. W. Perry. 2016. "Changing Disturbance Regimes, Ecological Memory, and Forest Resilience." Frontiers in Ecology and the Environment 14(7):369–78.

Jones, Matthew W., John T. Abatzoglou, Sander Veraverbeke, Niels Andela, Gitta Lasslop, Matthias Forkel, Adam J. P. Smith, Chantelle Burton, Richard A. Betts, and Guido R. van der Werf. 2022. "Global and Regional Trends and Drivers of Fire under Climate Change." Reviews of Geophysics 60(3):e2020RG000726.

Karpatne, Anuj, Imme Ebert-Uphoff, Sai Ravela, Hassan Ali Babaie, and Vipin Kumar. 2018. "Machine Learning for the Geosciences: Challenges and Opportunities." IEEE Transactions on Knowledge and Data Engineering 31(8):1544–54.

Keeley, Annika T. H., Paul Beier, and Jeff S. Jenness. 2021. "Connectivity Metrics for Conservation Planning and Monitoring." Biological Conservation 255:109008.

Keeley, Jon E., and Alexandra D. Syphard. 2016. "Climate Change and Future Fire Regimes: Examples from California." Geosciences 6(3):37.

Kelly, Luke T., and Lluís Brotons. 2017. "Using Fire to Promote Biodiversity." Science 355(6331):1264–65.

Kennedy, Robert E., Zhiqiang Yang, Noel Gorelick, Justin Braaten, Lucas Cavalcante, Warren B. Cohen, and Sean Healey. 2018. "Implementation of the LandTrendr Algorithm on Google Earth Engine." Remote Sensing 10(5):691.

Kim, Yunhee, Myeong-Hun Jeong, Minkyo Youm, Junkyeong Kim, and Jinpyung Kim. 2021. "Recovery of Forest Vegetation in a Burnt Area in the Republic of Korea: A Perspective Based on Sentinel-2 Data." Applied Sciences 11(6):2570.

Knorr, W., L. Jiang, and A. Arneth. 2016. "Climate, CO 2 and Human Population Impacts on Global Wildfire Emissions." Biogeosciences 13(1):267–82.

Kourtz, P. H. 1968. "Computers and Forest Fire Detection." The Forestry Chronicle 44(2):22–24.

Kustas, William, and Martha Anderson. 2009. "Advances in Thermal Infrared Remote Sensing for Land Surface Modeling." Agricultural and Forest Meteorology 149(12):2071–81.

Larson, Andrew J., Sean M. A. Jeronimo, Paul F. Hessburg, James A. Lutz, Nicholas A. Povak, C. Alina Cansler, Van R. Kane, and Derek J. Churchill. 2022. "Tamm Review: Ecological Principles to Guide Post-Fire Forest Landscape Management in the Inland Pacific and Northern Rocky Mountain Regions." Forest Ecology and Management 504:119680.

Learning, Deep. 2016. "Deep Learning-Goodfellow." Nature 26(7553):436.

LeCun, Yann, Yoshua Bengio, and Geoffrey Hinton. 2015. "Deep Learning." Nature 521(7553):436–44.

Libonati, R., J. M. C. Pereira, C. C. Da Camara, L. F. Peres, D. Oom, J. A. Rodrigues, F. L. M. Santos, R. M. Trigo, C. M. P. Gouveia, and F. Machado-Silva. 2021. "Twenty-First Century Droughts Have Not Increasingly Exacerbated Fire Season Severity in the Brazilian Amazon." Scientific Reports 11(1):4400.

Liu, Pengfei, Weiyu Zhuang, Weili Kou, Leiguang Wang, Qiuhua Wang, and Zhongjian Deng. 2025. "Fire Severity Outperforms Remote Sensing Indices in Exploring Post-Fire Vegetation Recovery Dynamics in Complex Plateau Mountainous Regions." Forests 16(2):263.

Llorens, Rafael, José Antonio Sobrino, Cristina Fernández, José M. Fernández-Alonso, and José Antonio Vega. 2021. "A Methodology to Estimate Forest Fires Burned Areas and Burn Severity Degrees Using Sentinel-2 Data. Application to the October 2017 Fires in the Iberian Peninsula." International Journal of Applied Earth Observation and Geoinformation 95:102243.

Lopes, Luis Filipe, Filipe S. Dias, Paulo M. Fernandes, and Vanda Acácio. 2024. "A Remote Sensing Assessment of Oak Forest Recovery after Postfire Restoration." European Journal of Forest Research 143(3):1001–14.

Marlon, Jennifer R., Patrick J. Bartlein, Christopher Carcaillet, Daniel G. Gavin, Sandy P. Harrison, Philip E. Higuera, Fortunat Joos, Mitchell J. Power, and I. C. Prentice. 2008. "Climate and Human Influences on Global Biomass Burning over the Past Two Millennia." Nature Geoscience 1(10):697–702.

Marlon, Jennifer R., Patrick J. Bartlein, Anne-Laure Daniau, Sandy P. Harrison, Shira Y. Maezumi, Mitchell J. Power, Willy Tinner, and Boris Vanniére. 2013. "Global Biomass Burning: A Synthesis and Review of Holocene Paleofire Records and Their Controls." Quaternary Science Reviews 65:5–25.

Martins, Bruno, Catarina Pinheiro, Adélia Nunes, António

Bento-Gonçalves, and Manuela Laranjeira. 2024. "Site-scale Drivers of Post-fire Vegetation Regrowth in Gullies: A Case Study in Mediterranean Europe." Earth Surface Processes and Landforms 49(13):4371–87.

McFeeters, Stuart K. 1996. "The Use of the Normalized Difference Water Index (NDWI) in the Delineation of Open Water Features." International Journal of Remote Sensing 17(7):1425–32.

Merrill, A. G., ANDREA E. Thode, ALEXANDRA M. Weill, J. A. Fites-Kaufman, ANNE F. Bradley, TADASHI J. Moody, J. W. Van Wagtendonk, N. G. Sugihara, S. L. Stephens, and K. E. Shaffer. 2018a. "Fire and Plant Interactions." Fire in California's Ecosystem. Second Edition. University of California Press, Oakland, California, USA 103–22.

Merrill, A. G., ANDREA E. Thode, ALEXANDRA M. Weill, J. A. Fites-Kaufman, ANNE F. Bradley, TADASHI J. Moody, J. W. Van Wagtendonk, N. G. Sugihara, S. L. Stephens, and K. E. Shaffer. 2018b. "Fire and Plant Interactions." Fire in California's Ecosystem. Second Edition. University of California Press, Oakland, California, USA 103–22.

NOAA. 2024. "NOAA 2024."

Pausas, Juli G., and Jon E. Keeley. 2019. "Wildfires as an Ecosystem Service." Frontiers in Ecology and the Environment 17(5):289–95.

Peel, M. C., B. L. Finlayson, and T. A. McMahon. 2007. "Updated World Map of the Köppen-Geiger Climate Classification." Hydrology and Earth System Sciences 11(5):1633–44. doi:10.5194/hess-11-1633-2007.

Priya, R. Shanmuga, and K. Vani. 2024. "Vegetation Change Detection and Recovery Assessment Based on Post-Fire Satellite Imagery Using Deep Learning." Scientific Reports 14(1):12611.

Qiu, Jie, Heng Wang, Wenjuan Shen, Yali Zhang, Huiyi Su, and Mingshi Li. 2021. "Quantifying Forest Fire and Post-Fire Vegetation Recovery in the Daxin'anling Area of Northeastern China Using Landsat Time-Series Data and Machine Learning." Remote Sensing 13(4):792.

Ramo, Rubén, and Emilio Chuvieco. 2017. "Developing a Random Forest Algorithm for MODIS Global Burned Area Classification." Remote Sensing 9(11):1193.

Reichstein, Markus, Gustau Camps-Valls, Bjorn Stevens, Martin Jung, Joachim Denzler, Nuno Carvalhais, and F. Prabhat. 2019. "Deep Learning and Process Understanding for Data-Driven Earth System Science." Nature 566(7743):195–204.

Rolnick, David, Priya L. Donti, Lynn H. Kaack, Kelly Kochanski, Alexandre Lacoste, Kris Sankaran, Andrew Slavin Ross, Nikola Milojevic-Dupont, Natasha Jaques, and Anna Waldman-Brown. 2022. "Tackling Climate Change with Machine Learning." ACM Computing Surveys (CSUR) 55(2):1–96.

RP, LIPPMAN. 1987. "An Introduction to Computing with Neural Nets." IEEE ASSP Magazine 4.

San-Miguel-Ayanz, Jesús, Tracy DURRANT, Roberto BOCA, Pieralberto MAIANTI, Giorgio LIBERTA, VIVANCOS Tomas ARTES, FELIX O. O. M. JACOME, Alfredo BRANCO, RIGO DE, and Davide FERRARI. 2022. "Advance Report on Wildfires in Europe, Middle East and North Africa 2021."

Shen, Chaopeng. 2018. "A Transdisciplinary Review of Deep Learning Research and Its Relevance for Water Resources Scientists." Water Resources Research 54(11):8558–93.

Simpson, Claire Emily, Morteza Karimzadeh, Jennifer Balch, and Danna Gurari. n.d. FORECASTING POST-FIRE VEGETATION RECOVERY DYNAMICS USING DEEP LEARNING AND REMOTE SENSING.

Souane, Ali Ahmed, Abbas Khurram, Hui Huang, Zhan Shu, Shujie Feng, Benamar Belgherbi, and Zhiyuan Wu. 2024. "Utilizing Machine Learning and Geospatial Techniques to Evaluate Post-Fire Vegetation Recovery in Mediterranean Forest Ecosystem: Tenira, Algeria." Forests 16(1):53.

Stathakis, Demetris, and Ioannis Kanellopoulos. 2008. "Global Elevation Ancillary Data for Land-Use Classification Using Granular Neural Networks." Photogrammetric Engineering & Remote Sensing 74(1):55–63.

Stathakis, Demetris, and Athanassios Vasilakos. 2006. "Comparison of Computational Intelligence Based Classification Techniques for Remotely Sensed Optical Image Classification." IEEE Transactions on Geoscience and Remote Sensing 44(8):2305–18.

Steel, Zachary L., Hugh D. Safford, and Joshua H. Viers. 2015. "The Fire Frequency-severity Relationship and the Legacy of Fire Suppression in California Forests." Ecosphere 6(1):1–23.

Stevens, Jens T., Hugh D. Safford, and Andrew M. Latimer. 2014. "Wildfire-Contingent Effects of Fuel Treatments Can Promote Ecological Resilience in Seasonally Dry Conifer Forests." Canadian Journal of Forest Research 44(8):843–54.

Stevens-Rumann, Camille S., Kerry B. Kemp, Philip E. Higuera, Brian J. Harvey, Monica T. Rother, Daniel C. Donato, Penelope Morgan, and Thomas T. Veblen. 2018. "Evidence for Declining Forest Resilience to Wildfires under Climate Change." Ecology Letters 21(2):243–52.

Sun, G. F., Xian-lin Qin, S. C. Liu, X. Li, X. Chen, and X. Zhong. 2019. "Potential Analysis of Typical Vegetation Index for Identifying Burned Area." Remote Sensing for Land and Resources 31(1):204–11.

Teshaev, Nozimjon, Aziz Inamov, and Kurbon Juraev. 2025. "Assessment of Forest Fires in Zaamin National Park Using Remote Sensing: Comparative Analysis of NBR and NDVI." P. 040042 in AIP Conference Proceedings. Vol. 3256. AIP Publishing LLC.

Toivonen, Janne, Annika Kangas, Matti Maltamo, Mikko Kukkonen, and Petteri Packalen. 2023. “Assessing Biodiversity Using Forest Structure Indicators Based on Airborne Laser Scanning Data.” Forest Ecology and Management 546:121376.

Tucker, Compton J. 1979. “Red and Photographic Infrared Linear Combinations for Monitoring Vegetation.” Remote Sensing of Environment 8(2):127–50.

Vanderhoof, Melanie K., Todd J. Hawbaker, Andrea Ku, Kyle Merriam, Erin Berryman, and Megan Cattau. 2021. “Tracking Rates of Postfire Conifer Regeneration vs. Deciduous Vegetation Recovery across the Western United States.” Ecological Applications 31(2):e02237.

Veraverbeke, S., S. Hook, and Glynn Hulley. 2012. “An Alternative Spectral Index for Rapid Fire Severity Assessments.” Remote Sensing of Environment 123:72–80.

Viedma, Olga, Nicolás Moity, and José M. Moreno. 2015. “Changes in Landscape Fire-Hazard during the Second Half of the 20th Century: Agriculture Abandonment and the Changing Role of Driving Factors.” Agriculture, Ecosystems & Environment 207:126–40.

Vlassova, Lidia, Fernando Pérez-Cabello, Marcos Rodrigues Mimbrero, Raquel Montorio Llovería, and Alberto García-Martín. 2014. “Analysis of the Relationship between Land Surface Temperature and Wildfire Severity in a Series of Landsat Images.” Remote Sensing 6(7):6136–62.

Wang, Lingli, and John J. Qu. 2007. “NMDI: A Normalized Multi-band Drought Index for Monitoring Soil and Vegetation Moisture with Satellite Remote Sensing.” Geophysical Research Letters 34(20).

Wang, Shuo, Xin Zheng, Yang Du, Guoqiang Zhang, Qianxue Wang, Daxiao Han, and Jili Zhang. 2025. “Estimation of Short-Term Vegetation Recovery in Post-Fire Siberian Dwarf Pine (Pinus Pumila) Shrublands Based on Sentinel-2 Data.” Fire 8(2):47.

Wassner, Noah, Albano Figueiredo, and Adélia N. Nunes. 2025. “Applying Remote Sensing to Assess Post-Fire Vegetation Recovery: A Case Study of Serra Do Açor (Portugal).” Fire 8(5):163.

Wilson, Natalie R., and Laura M. Norman. 2018. “Analysis of Vegetation Recovery Surrounding a Restored Wetland Using the Normalized Difference Infrared Index (NDII) and Normalized Difference Vegetation Index (NDVI).” International Journal of Remote Sensing 39(10):3243–74.

Xu, Xiao, Yating Li, Shuai Li, and Hui Fan. 2024. “Post-Fire Forest Recovery Trajectory Characterized by a Modified LandTrendr Recovery Detection Method: A Case Study of Pinus Yunnanensis Forests.” Agricultural and Forest Meteorology 354:110084.

Zahabnazouri, Somayeh, Patrick Belmont, Scott David, Peter E. Wigand, Mario Elia, and Domenico Capolongo. 2025. “Detecting Burn Severity and Vegetation Recovery After Fire Using DNBR and DNDVI Indices: Insight from the Bosco Difesa Grande, Gravina in Southern Italy.” Sensors 25(10):3097.

Zhang, Qiyue, Saeid Homayouni, Pengwu Zhao, and Mei Zhou. 2023. “Burned Vegetation Recovery Trajectory and Its Driving Factors Using Satellite Remote-Sensing Datasets in the Great Xing’An Forest Region of Inner Mongolia.” International Journal of Wildland Fire 32(2):244–61.

Zhijie, Zhu. 2024. “Advancements in Forest Fire Monitoring and Management: Insights from Canadian Research and Global Perspectives.” Journal of Natural and Life Sciences.(1) 20–24.

Zou, Yufei, Yuhang Wang, Yun Qian, Hanqin Tian, Jia Yang, and Ernesto Alvarado. 2020. “Using CESM-RESFire to Understand Climate–Fire–Ecosystem Interactions and the Implications for Decadal Climate Variability.” Atmospheric Chemistry and Physics 20(2):995–1020.